

This discussion paper is/has been under review for the journal Atmospheric Chemistry and Physics (ACP). Please refer to the corresponding final paper in ACP if available.

Aerosol mass spectrometer constraint on the global secondary organic aerosol budget

D. V. Spracklen¹, J. L. Jimenez², K. S. Carslaw¹, D. R. Worsnop³, M. J. Evans¹, G. W. Mann¹, Q. Zhang⁴, M. R. Canagaratna³, J. Allan⁵, H. Coe⁵, G. McFiggans⁵, A. Rap¹, and P. Forster¹

¹School of Earth and Environment, University of Leeds, Leeds, LS2 9JT, UK

²Department of Chemistry and Biochemistry, and CIRES, University of Colorado, Boulder, CO, USA

³Aerodyne Research, Billerica, MA, USA

⁴Department of Environmental Toxicology, University of California, Davis, CA, USA

⁵Centre for Atmospheric Science, School of Earth, Atmospheric and Environmental Sciences, University of Manchester, Manchester, UK

Received: 29 December 2010 – Accepted: 1 February 2011 – Published: 16 February 2011

Correspondence to: D. V. Spracklen (dominick@env.leeds.ac.uk)

Published by Copernicus Publications on behalf of the European Geosciences Union.

[Title Page](#)

[Abstract](#)

[Introduction](#)

[Conclusions](#)

[References](#)

[Tables](#)

[Figures](#)

[◀](#)

[▶](#)

[Back](#)

[Close](#)

[Full Screen / Esc](#)

[Printer-friendly Version](#)

[Interactive Discussion](#)



Abstract

The budget of atmospheric secondary organic aerosol (SOA) is very uncertain, with recent estimates suggesting a global source of between 12 and 1820 Tg (SOA) a^{-1} . We used a dataset of aerosol mass spectrometer (AMS) observations and a global chemical transport model including aerosol microphysics to produce top-down constraints on the SOA budget. We treated SOA formation from biogenic (monoterpenes and isoprene), lumped anthropogenic and lumped biomass burning volatile organic compounds (VOCs) and varied the SOA yield from each precursor source to produce the best overall match between model and observations. Organic aerosol observations from the IMPROVE network were used as an independent check of our optimised sources. The optimised model has a global SOA source of 140 ± 90 Tg (SOA) a^{-1} comprised of 13 ± 8 Tg (SOA) a^{-1} from biogenic, 100 ± 60 Tg (SOA) a^{-1} from anthropogenically controlled SOA, 23 ± 15 Tg (SOA) a^{-1} from conversion of primary organic aerosol (mostly from biomass burning) to SOA and an additional 3 ± 3 Tg (SOA) a^{-1} from biomass burning VOCs. Compared with previous estimates, our optimized model has a substantially larger SOA source in the Northern Hemisphere mid-latitudes. We used a dataset of ^{14}C observations from rural locations to estimate that 10 Tg (SOA) a^{-1} (10%) of our anthropogenically controlled SOA is of urban/industrial origin, with 90 Tg (SOA) a^{-1} (90%) most likely due to an anthropogenic pollution enhancement of SOA from biogenic VOCs, almost an order-of-magnitude beyond what can be explained by current understanding. The urban/industrial SOA source is consistent with the $13\text{ Tg }a^{-1}$ estimated by de Gouw and Jimenez (2009), which was much larger than estimates from previous studies. The anthropogenically controlled SOA source results in a global mean aerosol direct effect of $-0.26 \pm 0.15\text{ W m}^{-2}$ and global mean indirect (cloud albedo) effect of $-0.6_{-0.14}^{+0.24}\text{ W m}^{-2}$. The biogenic and biomass SOA sources are not well constrained due to the limited number of OA observations in regions and periods strongly impacted by these sources. To further improve the constraints by this method, additional observations are needed in the tropics and the Southern Hemisphere.

Aerosol mass spectrometer constraint on the global SOA budget

D. V. Spracklen et al.

[Title Page](#)

[Abstract](#)

[Introduction](#)

[Conclusions](#)

[References](#)

[Tables](#)

[Figures](#)

◀

▶

[Back](#)

[Close](#)

[Full Screen / Esc](#)

[Printer-friendly Version](#)

[Interactive Discussion](#)



1 Introduction

Organic aerosol (OA) contributes about 50% of dry tropospheric submicron aerosol mass (Putaud et al., 2004; Murphy et al., 2006; Zhang et al., 2007) with important impacts on climate (Forster et al., 2007) and air quality. OA sources can be split into primary organic aerosol (POA) that is emitted directly to the atmosphere as particles, and secondary organic aerosol (SOA) that forms in the atmosphere from gas-to-particle conversion. The global budget of SOA is very uncertain. Recent top-down estimates, based either on the mass balance of volatile organic carbon (VOC) or on scaling of the sulfate budget, suggest a global source ranging from 120–1820 Tg (SOA) a^{-1} (Goldstein and Galbally, 2007; Hallquist et al., 2009)¹. Meanwhile atmospheric models typically use bottom-up estimates which combine emission inventories for VOCs with laboratory based SOA yields to give a global SOA formation of 12–70 Tg (SOA) a^{-1} (Kanakidou et al., 2005).

In addition to the total budget of SOA being highly uncertain, the relative contributions from anthropogenic, biogenic, and biomass burning sources are also poorly constrained. Regional and global atmospheric models using “traditional” SOA parameterizations (those developed until 2006) formed SOA mostly from biogenic VOCs and typically showed large SOA underestimations in polluted regions (e.g. Heald et al., 2005; Volkamer et al., 2006; Hodzic et al., 2010a) but not for clean biogenic regions (Tunved et al., 2006; Chen et al., 2009; Hodzic et al., 2009; Slowik et al., 2010). Recently, formation of SOA from additional sources has been included in models. Several box (Dzepina et al., 2009), regional (Hodzic et al., 2010a; Tsimpidi et al., 2010) and global (Pye and Seinfeld, 2010) modelling studies have explored enhanced formation of SOA from semivolatile and intermediate volatility organic compounds (S/IVOC), which are SOA precursors emitted by anthropogenic and biomass burning sources (Robinson et al., 2007). These studies reported that such precursors may be an important

¹We assume a conversion factor of 2 Tg (SOA)/Tg (C) over space and time scales relevant to global models (Turpin and Lim, 2001; Aiken et al., 2008).

Aerosol mass spectrometer constraint on the global SOA budget

D. V. Spracklen et al.

[Title Page](#)

[Abstract](#)

[Introduction](#)

[Conclusions](#)

[References](#)

[Tables](#)

[Figures](#)

◀

▶

[Back](#)

[Close](#)

[Full Screen / Esc](#)

[Printer-friendly Version](#)

[Interactive Discussion](#)



and previously neglected regional and global SOA source. However, there is still substantial uncertainty in the concentrations, reaction rates, and SOA yields of S/I VOC precursors. Some new parameterizations of SOA formation from anthropogenic VOCs (Lane et al., 2008; Tsimpidi et al., 2010) result in very high mass yields (e.g. ~100% for toluene after ~3 days, Dzepina et al., 2010), but are not yet fully supported by laboratory data. SOA formed from biomass burning precursors is gaining attention as a potentially important source, although both field (Capes et al., 2008; Yokelson et al., 2009; DeCarlo et al., 2010) and laboratory (Grieshop et al., 2009) studies appear to show high variability in the net addition (or sometimes loss) of OA mass due to SOA formation and POA aging from this source.

At the global scale, modelling studies using early SOA models predict that the formation of SOA from biogenic sources greatly exceeds that from anthropogenic sources (Tsigaridis et al., 2006; Tsigaridis and Kanakidou, 2007; Heald et al., 2008; Henze et al., 2008), while newer models predict a larger share for anthropogenic SOA (Farina et al., 2010, Pye and Seinfeld, 2010). The importance of biogenic SOA appears to be consistent with the large fraction of non-fossil carbon detected in ambient OA (e.g., Hodzic et al., 2010b). Even in polluted regions, where concentrations of OA are enhanced, substantial fractions of non-fossil carbon are detected (e.g., Schichtel et al., 2008) leading to the suggestion that biogenic SOA formation may be enhanced by anthropogenic pollution (de Gouw et al., 2005; Weber et al., 2007). Potential mechanisms for such enhanced formation include higher aerosol acidity (e.g. Jang et al., 2002; Surratt et al., 2010, Froyd et al., 2010), NO_x levels (Kroll et al., 2006) and speciation (e.g. Chan et al., 2010), enhanced pollution-related OA and oxidant levels (Tsigaridis and Kanakidou, 2007), and oxidant speciation (e.g. Ng et al., 2008). A recent study predicted a factor of 2 enhancement of biogenic SOA by pollution in the US, due primarily to increased NO_x concentrations that enhance biogenic VOC oxidation, and through anthropogenic POA acting as a medium for adsorption of condensable species of biogenic origin (Carlton et al., 2010). Not all of the observed non-fossil carbon is due to biogenic SOA, however, as important contributions also arise due to biomass burning,

Aerosol mass spectrometer constraint on the global SOA budget

D. V. Spracklen et al.

[Title Page](#)

[Abstract](#)

[Introduction](#)

[Conclusions](#)

[References](#)

[Tables](#)

[Figures](#)

◀

▶

◀

▶

[Back](#)

[Close](#)

[Full Screen / Esc](#)

[Printer-friendly Version](#)

[Interactive Discussion](#)



biofuel use, and of non-fossil urban OA sources (Hodzic et al., 2010b; Hildemann et al., 1994).

In this paper we use a global aerosol microphysics model and a global dataset of OA observations to produce a new top-down constraint on the total and source-specific global SOA budget. The different sources are parameterized based on results from recent field measurement campaigns using aerosol mass spectrometry, and the optimum is found by adjusting the strength of the different sources until the model/measurement error is minimized. We use OA observations from the IMPROVE network over the United States to test our optimised sources and a dataset of ^{14}C observations to evaluate our source-specific SOA budget.

2 Methods

2.1 GLOMAP global aerosol model

We used the Global Model of Aerosol Processes (GLOMAP) (Spracklen et al., 2005a, b) which is an extension of the TOMCAT 3-D global chemical transport model (Chipperfield, 2006). We used the modal version of the model (GLOMAP-mode) where the aerosol size distribution is treated using a two-moment modal scheme (Manktelow et al., 2007; Mann et al., 2010). We simulated sulfate, sea-salt, elemental carbon, POA and SOA as distinct aerosol components and simulated the aerosol size distribution with 5 modes: hygroscopic nucleation, Aitken, accumulation and coarse modes plus a non-hygroscopic Aitken mode. We do not treat dust, ammonium or nitrate aerosol. The model was run for the year 2000 using a horizontal resolution of $\sim 2.8^\circ \times 2.8^\circ$ and with 31 vertical levels between the surface and 10 hPa.

The model described in Mann et al. (2010) only includes SOA from monoterpenes. For this study we implemented a new SOA scheme in the model. We included SOA formation from 4 VOC classes: monoterpenes, isoprene, lumped anthropogenic VOCs (VOC_A) and lumped biomass burning VOCs (VOC_BB). Throughout the paper we term

[Title Page](#)[Abstract](#)[Introduction](#)[Conclusions](#)[References](#)[Tables](#)[Figures](#)[◀](#)[▶](#)[Back](#)[Close](#)[Full Screen / Esc](#)[Printer-friendly Version](#)[Interactive Discussion](#)

the SOA that is linked to anthropogenic VOC emissions as “anthropogenically controlled” to underscore the fact that it likely to be a combination of SOA formed directly from oxidation of anthropogenic VOCs as well as potentially from enhancement of biogenic SOA production due to anthropogenic pollution. In a set of sensitivity simulations we allowed POA to convert directly to SOA with a half life which we set at between 1 and 8 days. Much of this POA aging is thought to occur via the gas-phase (Robinson et al., 2007) and thus the processed material can be correctly referred to as SOA. Some of the POA may be oxidized heterogeneously in the particle phase, especially at very long aging times (George and Abbatt, 2010), and would more correctly be referred to as oxidized POA.

Emissions of POA from fossil fuel ($3.2 \text{ Tg(OA) a}^{-1}$), biofuel ($9.1 \text{ Tg(OA) a}^{-1}$) and wildfire ($34.7 \text{ Tg(OA) a}^{-1}$) are from the AEROCOM inventory (Dentener et al., 2006). Emissions of monoterpenes and isoprene were taken from the Global Emissions Inventory Activity (GEIA), based on Guenther et al. (1995). For emissions of VOC_A and VOC_{BB} we scaled gridded CO emissions from the IPCC. This scaling is supported by the very frequently observed proportionality of SOA formation to CO in polluted regions (e.g., de Gouw et al., 2008; Dzepina et al., 2009; de Gouw and Jimenez, 2009; DeCarlo et al., 2010). IPCC CO emissions from anthropogenic activity ($470.5 \text{ Tg(CO) a}^{-1}$) and biomass burning ($507.5 \text{ Tg(CO) a}^{-1}$) were scaled using VOC/CO mass ratios of 0.29 g/g and 0.10 g/g respectively so as to reproduce the global sum of VOC emissions from the Emissions Database for Atmospheric Research (EDGAR) for anthropogenic ($127 \text{ Tg(VOC) a}^{-1}$) and biomass burning ($49 \text{ Tg(VOC) a}^{-1}$) sources.

We included reactions of monoterpenes and isoprene with OH, O_3 and NO_3 , and reactions of VOC_A and VOC_{BB} with OH (Table 1). For the reactions of VOC_A and VOC_{BB} we tested the sensitivity to changes in the reaction rate. Concentrations of oxidants were specified using 6-hourly monthly mean 3-D gridded concentration fields from a TOMCAT simulation with detailed tropospheric chemistry (Arnold et al., 2005). Figure 1 shows simulated surface concentrations of the different VOCs.

Aerosol mass spectrometer constraint on the global SOA budget

D. V. Spracklen et al.

[Title Page](#)

[Abstract](#)

[Introduction](#)

[Conclusions](#)

[References](#)

[Tables](#)

[Figures](#)

◀

▶

◀

▶

[Back](#)

[Close](#)

[Full Screen / Esc](#)

[Printer-friendly Version](#)

[Interactive Discussion](#)



Condensable gas-phase species (including VOC oxidation products and H₂SO₄) are allowed to condense on all aerosol modes. In all simulations we assume an SOA/OC mass ratio of 2.0. To reduce the computational burden of our simulations, we assumed the first-step oxidation product of the above reactions condenses kinetically, and irreversibly, as SOA with negligible vapour pressure onto pre-existing aerosol. Although fresh SOA is known to be semivolatile (Odum et al., 1996; Cappa and Jimenez, 2010), it has been recently shown that aged SOA has low volatility (Jimenez et al., 2009; Cappa and Jimenez, 2010) and may form a highly viscous glassy state (Virtanen et al., 2010; Cappa and Wilson, 2010), which is likely to be most relevant to the time and length scales of our global modelling study. Additionally, we have previously shown that kinetic uptake of SOA onto pre-existing aerosol allows the model to simulate the growth of newly formed particles in the 3 to 100 nm size range (Spracklen et al., 2006, 2008a). But we note that volatility is a further free parameter in the model that should be investigated in the future.

We do not include an OA source from the oceans (e.g., Spracklen et al., 2008b) because the size distribution of the source is not well known and it is not clear what fraction of this source is primary as opposed to secondary. Oceanic isoprene emissions are thought to be <1% of the terrestrial source (Arnold et al., 2009) while the monoterpene source is very uncertain (Yassa et al., 2008). Since the concentrations of OA arising from the marine source are generally low in comparison to continental regions (Spracklen et al., 2008b) and since the majority of the AMS observations used here are from continental locations this is unlikely to be an issue in our analysis.

2.2 SOA simulations

We conducted a set of annual simulations (detailed in Table 2) where we varied the sources of SOA. In each set of simulations that are described below, the source of SOA from the VOC precursors was varied by altering the yield (y_1 to y_{10}) of the reactions in Table 1. The source of SOA from ageing of POA was altered by changing the lifetime of conversion of POA to SOA. The upper limit for each source was chosen where an

[Title Page](#)[Abstract](#)[Introduction](#)[Conclusions](#)[References](#)[Tables](#)[Figures](#)[◀](#)[▶](#)[Back](#)[Close](#)[Full Screen / Esc](#)[Printer-friendly Version](#)[Interactive Discussion](#)

increase in the source did not result in better agreement with the AMS observations that are described in the following section. In the first set of model experiments (simulations 1–5) we included SOA formation from monoterpenes ($0\text{--}246 \text{Tg (SOA) a}^{-1}$) and isoprene ($0\text{--}52 \text{Tg (SOA) a}^{-1}$). The standard model (Mann et al., 2010, simulation 1) only includes SOA from monoterpenes. In the second set of experiments (simulations 6–7) we included SOA formation from biomass burning VOCs ($0\text{--}212 \text{Tg (SOA) a}^{-1}$). In the third set of experiments (simulations 8–10) we included SOA from ageing of POA ($0\text{--}79 \text{Tg (SOA) a}^{-1}$). In the fourth set of experiments (simulations 11–24) we included SOA from anthropogenic VOCs ($0\text{--}117 \text{Tg (SOA) a}^{-1}$). In a final set of experiments we tested a number of potential mechanisms under which formation of SOA from biogenic VOCs could be enhanced by anthropogenic pollution. We altered the SOA yield from monoterpenes separately with OH, O₃ and NO₃ (simulations 25–27), included SO₂ catalysed formation of SOA from isoprene and monoterpenes (simulations 28–29, as a representation of acid-catalysed biogenic SOA formation) and included VOC_A catalysed formation of SOA from isoprene and monoterpenes (simulations 30–33, as a representation of biogenic SOA enhancement by anthropogenic pollutants with similar emission pattern as fossil fuel CO and lifetime similar to our assumed VOC_A).

2.3 AMS observations

We compared GLOMAP against a data set of OA measurements from the aerosol mass spectrometer (AMS). The AMS has been described in detail previously (Canagaratna et al., 2007), and provides fast on-line submicron non-refractory (NR) aerosol composition. NR is operationally defined based on evaporation under a few seconds under the AMS conditions (600 °C, high vacuum) and in practice includes organic species and most inorganic salts and excludes black carbon, mineral dust, and sea salt. Factor analysis of AMS spectra allows the identification of OA components, principally hydrocarbon-like OA (HOA, a surrogate for combustion POA, and here also including primary biomass burning OA, P-BBOA) and oxygenated OA (OOA, a surrogate for SOA from all sources). Based on many recent observations (e.g. Zhang et al., 2005;

[Title Page](#)[Abstract](#)[Introduction](#)[Conclusions](#)[References](#)[Tables](#)[Figures](#)[◀](#)[▶](#)[Back](#)[Close](#)[Full Screen / Esc](#)[Printer-friendly Version](#)[Interactive Discussion](#)

Lanz et al., 2007; Dzepina et al., 2009; Aiken et al., 2008, 2009), we assumed that simulated POA (including that from biomass burning) is equivalent to observed HOA and that simulated SOA (and including SOA formed from oxidised POA where this was treated in the model) is equivalent to observed OOA.

We supplemented the dataset of AMS observations compiled by Zhang et al. (2007) with 10 more recent observations (Table 3) giving a total of 47 average observations. Each observation is typically the average of ~1 month of continuously sampled data at ground locations. The majority of our observations are near sea-level and in the boundary layer (BL). A few observations are from high-altitude sites which may sample free tropospheric air for parts of the observation period. We included 4 observations from aircraft where these extended the geographical spread of our dataset. For these experiments we report the average of the BL data. Our dataset has limited information on the concentrations of OA above the BL. Since recent aircraft observations (Heald et al., 2006; Dunlea et al., 2009) do not suggest a major SOA source in the FT this should not greatly impact our analysis. However, additional information on the vertical profile of OA is important in reducing the uncertainty in the OA budget. Whereas the Zhang et al. (2007) database was limited to the Northern Hemisphere (NH) extra-tropics (19° N to 62° N) our new dataset includes observations both in the Southern Hemisphere and tropics (19° S to 62° N) which as we show below, are important in constraining the global SOA source. As in Zhang et al. (2007) all sites are classified as urban, urban-downwind or remote.

2.4 IMPROVE observations

As an independent test of our optimised SOA sources we also compared the model against organic carbon (OC) concentrations measured by the Interagency Monitoring of Protected Visual Environments (IMPROVE) network (Malm et al., 1994). We used observed monthly mean IMPROVE concentrations for the year 2000, which is the year simulated by the model. We also compared against the multi-year (2000–2004) IMPROVE monthly mean observations. In the year 2000 there were 108 IMPROVE

[Title Page](#)[Abstract](#)[Introduction](#)[Conclusions](#)[References](#)[Tables](#)[Figures](#)[◀](#)[▶](#)[Back](#)[Close](#)[Full Screen / Esc](#)[Printer-friendly Version](#)[Interactive Discussion](#)

stations that reported OC. We linearly interpolated monthly mean model output to the location of the IMPROVE observations.

3 Results

3.1 Global model simulations

- 5 For each of the global model simulations in Table 2 we spatially and temporally interpolated monthly mean component-resolved aerosol mass concentrations to the location and time period of the AMS observations. Table 2 summarises normalised mean bias (NMB), normalised mean error (NME) and correlation coefficient (r^2) between model and observations. Figure 2 shows sulfate, OA, HOA and OOA ob-
10 served by the AMS against the standard version of the global model (simulation 1, SOA from monoterpenes only). The model reasonably captures the observed distribution of sulfate (NMB = 18%, NME = 66%, r^2 = 0.36) but underpredicts OA (NMB = -68%, NME = 74%, r^2 = 0.27), HOA (NMB = -16%, NME = 85%, r^2 = 0.27) and OOA (NMB = -85%, NME = 87%) concentrations and has no skill in capturing
15 the spatial pattern of OOA (r^2 = 0.0). Model underprediction of HOA is driven by an underprediction at urban locations, most likely because the spatial resolution of the global model is too coarse to resolve urban-scale pollution. The model overpredicts HOA at remote locations which we discuss below. Average OOA concentrations at some remote sites (e.g., Central Amazon (AMAZE), north-eastern North America
20 (White Face Mountain, Chebogue Point), West Africa (AMMA)) are reasonably simulated (within a factor 2) although OOA is underpredicted on average across all remote sites (NMB = -80%).

We completed 5 sets of simulations where we varied the SOA formation from the 5 different sources as described in Sect. 2.2. We tested each simulation against ob-
25 served concentrations of OOA using NME and r^2 as an indicator of model skill. First, we modified the source of SOA from isoprene and monoterpenes (Fig. 3). Increasing

[Title Page](#)[Abstract](#)[Introduction](#)[Conclusions](#)[References](#)[Tables](#)[Figures](#)[◀](#)[▶](#)[Back](#)[Close](#)[Full Screen / Esc](#)[Printer-friendly Version](#)[Interactive Discussion](#)

the source of SOA from monoterpenes (simulations 2–3) or isoprene (simulations 4–5) reduces the model bias but does not improve model skill. For example, the model simulation where we increased the SOA yield from monoterpenes to 130%, from 26% in the standard simulation, resulting in a global SOA source of $161.5 \text{ Tg (SOA) a}^{-1}$, reduces the bias ($\text{NMB} = -24\%$) but model skill is not improved ($\text{NME} = 94\%$, $r^2 = 0.0$). Further increasing the SOA yield from monoterpenes to 198%, resulting in a global SOA source of $246 \text{ Tg (SOA) a}^{-1}$, results in an overprediction of SOA on average across all the sites ($\text{NMB} = 16\%$) and unimproved model skill ($\text{NME} = 118\%$, $r^2 = 0.0$). These simulations suggest that a monoterpene SOA source of $\sim 210 \text{ Tg (SOA) a}^{-1}$ would be sufficient to match the average magnitude of the AMS observations (i.e., reduce mean model bias to zero), but would not improve model skill. Similarly, including SOA from isoprene (assuming an SOA yield of 6% or 12%) reduces the model bias ($\text{NMB} = -68\%$ and $= 63\%$ respectively) but does not improve model skill ($\text{NME} = 85\%$, $r^2 = 0.0$). These results suggest that an increase of biogenic SOA alone is unable to explain the spatial and temporal patterns in the global OOA observations and additional SOA sources with a different spatial and temporal behaviour must exist to explain the observations.

In the second set of experiments (simulations 6–7) we included an additional SOA source from biomass burning (Fig. 4), which in the baseline run was set to zero. Assuming an SOA yield of 90% from biomass burning VOCs (simulation 6), resulting in an SOA source of $42.3 \text{ Tg (SOA) a}^{-1}$, leads to a reduction in model bias ($\text{NMB} = -71\%$) and improves model skill ($\text{NME} = 81\%$, $r^2 = 0.03$). However, further increasing the SOA yield from biomass burning VOCs to 180% (simulation 7, $84.6 \text{ Tg (SOA) a}^{-1}$) resulted in no further reduction in model error ($\text{NME} = 81\%$, $r^2 = 0.03$).

The third set of experiments (simulations 8–10) tests the effect of an additional source of OOA through oxidation of POA. At remote sites, where observed HOA concentrations were below the detection limit, the baseline model overpredicts HOA concentrations ($\text{NMB} = 274\%$). This overprediction could be due to heterogeneous oxidation of HOA to OOA that is not treated in the baseline simulations, underprediction of HOA removal by wet or dry deposition, or the uncertainty in accurately extracting a

Aerosol mass spectrometer constraint on the global SOA budget

D. V. Spracklen et al.

[Title Page](#)

[Abstract](#)

[Introduction](#)

[Conclusions](#)

[References](#)

[Tables](#)

[Figures](#)

◀

▶

◀

▶

[Back](#)

[Close](#)

[Full Screen / Esc](#)

[Printer-friendly Version](#)

[Interactive Discussion](#)



Aerosol mass spectrometer constraint on the global SOA budget

D. V. Spracklen et al.

[Title Page](#)[Abstract](#)[Introduction](#)[Conclusions](#)[References](#)[Tables](#)[Figures](#)[Back](#)[Close](#)[Full Screen / Esc](#)[Printer-friendly Version](#)[Interactive Discussion](#)

Finally, in the fifth set of experiments (simulations 24–32) we examined a number of simple mechanisms to parameterize a possible enhancement of biogenic SOA by anthropogenic pollution. We found that there was no improvement in model skill when we increased the monoterpene SOA yield to 130% individually for reaction with NO_3 (simulation 24, NME = 85%, $r^2 = 0.0$), O_3 (simulation 25, NME = 85%, $r^2 = 0.0$) or OH (simulation 26, NME = 83%, $r^2 = 0.0$). Including a reaction that represented acid-catalysed production of SOA from biogenic VOCs (simulations 27–28) results in a slight improvement in model skill (NME = 80%, $r^2 = 0.0$). Including a reaction that represents anthropogenic pollution catalysis of biogenic SOA (simulations 29–32) also results in a slight improvement in model skill (NME = 80%, $r^2 = 0.01$). However, the comparison between model and observations was substantially poorer than in simulations where the SOA source was linked directly to anthropogenic CO emissions. It is important to stress that we do not suggest that this simple empirical scheme where a source of SOA is linked to CO emissions describes the mechanism behind SOA formation.

Of the global model simulations we completed, the best fit with observations (simulation, 16, NMB = -23%, NME = 50%, $r^2 = 0.25$) is with an anthropogenically controlled SOA source of $114 \text{ Tg(SOA)} \text{ a}^{-1}$ and no SOA from other sources. The agreement with this simulation is even better when considering only remote sites (NMB = -10%, NME = 41%, $r^2 = 0.51$) demonstrating that the anthropogenically controlled SOA source improves simulated OOA in remote as well as polluted urban locations. However, without any biogenic or biomass SOA sources, the concentrations of OOA during AMAZE are underpredicted by almost a factor 10. In the next section we use the global model simulations to optimise the SOA sources.

3.2 Optimisation of the SOA source

Due to computational constraints it is not possible to run the global model enough times to be able to accurately quantify the SOA sources that result in the optimum match with the AMS observations. Therefore to optimise the SOA sources we created linear

[Title Page](#)[Abstract](#)[Introduction](#)[Conclusions](#)[References](#)[Tables](#)[Figures](#)[◀](#)[▶](#)[Back](#)[Close](#)[Full Screen / Esc](#)[Printer-friendly Version](#)[Interactive Discussion](#)

parameterisations of the global model which were computationally cheap and could be used to simulate SOA for a very large combination of SOA sources. In Sect. 3.5 we test the SOA sources optimised here in the full global model to confirm that they improve simulation of the AMS observations.

The linear models simulate SOA as a function of the 5 different SOA sources. We created a separate linear model for each of the 47 AMS observations in our dataset. We used as input the global model simulations 1–17 that are detailed in Table 2. We do not include simulations 18–33 as these simulations did not result in improved model skill. SOA simulated by each global model simulation was interpolated to the location and time period of the AMS observation as in Sect. 3.1. At each AMS location we then calculated a multiple linear fit of the interpolated SOA (SOA_int) simulated by the 17 global simulations as a function of the 5 different SOA sources: monoterpene (S_M), isoprene (S_I), anthropogenic (S_A), biomass burning (S_{BB}) and ageing of POA (S_P) resulting in a linear equation of the form:

SOA_int = $a \times S_M + b \times S_I + c \times S_A + d \times S_{BB} + e \times S_P + f$,

where a , b , c , d and e are the regression coefficients and f is the error term. Each linear equation was then used to calculate simulated SOA at that location. We ran each of the 47 models over same range of SOA sources simulated by the global model but at much finer increments in SOA source and over the full combination of the 5 different sources. For each combination of the SOA sources we then calculated the NME between the SOA simulated by the 47 models and the AMS observations at the 47 locations.

Figure 5 a, b shows NME between SOA simulated by the linear models and OOA observed by the AMS as a function of SOA source. The NME is calculated across all AMS locations. The minimum in NME between simulated and observed SOA is 47.5%. To calculate the optimum SOA source we first calculated the array of SOA sources that result in a NME that was within 2% of minimum NME (in this case a NME less than 48.5%). We assumed that the optimised SOA source was the average of the array

Aerosol mass spectrometer constraint on the global SOA budget

D. V. Spracklen et al.

[Title Page](#)

[Abstract](#)

[Introduction](#)

[Conclusions](#)

[References](#)

[Tables](#)

[Figures](#)

◀

▶

[Back](#)

[Close](#)

[Full Screen / Esc](#)

[Printer-friendly Version](#)

[Interactive Discussion](#)



that satisfied this criteria. We tested the sensitivity of our optimisation method to a range of cutoff values from within 0.5% of the minimum in NME (in this case a NME less than 47.7%) to within 5% (in this case a NME less than 50%) and found that this altered our total optimised SOA source by less than 5%. For the rest of the work we used a cutoff value of 2%. We assume that the error in our fitting method was equal to the standard deviation of the array of SOA sources that satisfy the above criteria. The relative error in the different sources of SOA was isoprene: $\pm 92\%$; monoterpene: $\pm 92\%$; anthropogenically controlled: $\pm 4\%$; biomass burning: $\pm 22\%$; POA to OOA conversion: 25%.

Using the method described above gives an optimised SOA source of $130 \pm 4 \text{ Tg (SOA) } a^{-1}$, consisting of $1 \pm 1 \text{ Tg (SOA) } a^{-1}$ from isoprene, $1 \pm 1 \text{ Tg (SOA) } a^{-1}$ from monoterpene, $2 \pm 0.4 \text{ Tg (SOA) } a^{-1}$ from biomass burning, $95 \pm 4 \text{ Tg (SOA) } a^{-1}$ from anthropogenically controlled SOA and $30 \pm 20 \text{ Tg (SOA) } a^{-1}$ from POA to OOA conversion. We also optimised the model against both OOA and total OA. This did not impact our optimised source greatly: our optimised total SOA source was $135 \pm 4 \text{ Tg (SOA) } a^{-1}$, consisting of $1 \pm 1 \text{ Tg (SOA) } a^{-1}$ from isoprene, $1 \pm 1 \text{ Tg (SOA) } a^{-1}$ from monoterpene, $2 \pm 0.4 \text{ Tg (SOA) } a^{-1}$ from biomass burning, $100 \pm 4 \text{ Tg (SOA) } a^{-1}$ from anthropogenically controlled SOA and $30 \pm 8 \text{ Tg (SOA) } a^{-1}$ from POA to OOA conversion.

The quoted uncertainties above only include uncertainty in our fitting process. Our simulated SOA budget is also uncertain due to errors in OA and OOA observed by the AMS, OA aerosol lifetime simulated by the global model and the vertical profile of OA simulated by the global model. We estimated the uncertainty arising due to each of these factors. We estimated an AMS observation uncertainty of $\pm 25\%$ (Canagaratna et al., 2007), which is consistent with the agreement we show below between the optimised model and the IMPROVE observations. The AEROCOM multi-model OA lifetime (mean \pm standard deviation) is $6.54 \text{ days} \pm 27\%$ (Textor et al., 2006) and is well matched by the lifetime in GLOMAP (6.1 days, Mann et al., 2010). We assumed that this standard deviation in AEROCOM multi-model lifetime is representative

Aerosol mass spectrometer constraint on the global SOA budget

D. V. Spracklen et al.

[Title Page](#)

[Abstract](#)

[Introduction](#)

[Conclusions](#)

[References](#)

[Tables](#)

[Figures](#)

◀

▶

◀

▶

[Back](#)

[Close](#)

[Full Screen / Esc](#)

[Printer-friendly Version](#)

[Interactive Discussion](#)



of the uncertainty in simulated aerosol lifetime. The simulated vertical profile of OA is not well constrained due to a limited number of AMS observations above the BL. We estimated that uncertainty in the vertical profile introduces a $\pm 50\%$ uncertainty in our optimised SOA budget. We combined these errors with the errors in our fitting technique in quadrature. This gave an overall error in total SOA source of $\pm 62\%$ with errors in the individual sources of isoprene: 110%, monoterpenes: 110%, biomass burning: 66%, POA to SOA conversion: 66%, anthropogenically controlled: 62%. Our optimised SOA source, with our full uncertainty estimate, is $130 \pm 80 \text{ Tg (SOA) a}^{-1}$, consisting of $1 \pm 1 \text{ Tg (SOA) a}^{-1}$ from isoprene, $1 \pm 1 \text{ Tg (SOA) a}^{-1}$ from monoterpenes, $2 \pm 3 \text{ Tg (SOA) a}^{-1}$ from biomass burning, $95 \pm 60 \text{ Tg (SOA) a}^{-1}$ from anthropogenically controlled SOA and $30 \pm 20 \text{ Tg (SOA) a}^{-1}$ from POA to OOA conversion.

3.3 Representativeness of AMS dataset

The AMS observations used in our analysis are not equally distributed around the globe since the majority of observations were made during the summer in the NH mid-latitudes. This unequal distribution may introduce a bias into our optimised SOA sources. To explore this possibility we tested how representative the AMS dataset was in terms of the concentration probability distribution of the different VOCs in our SOA scheme. Because coincident AMS and VOC observations are rarely available we were not able to compare simulated versus observed VOC concentrations at the AMS locations. Instead we compared the GLOMAP simulated probability distribution of VOC concentrations over all continental locations (excluding Antarctica) against the GLOMAP simulated probability distribution of VOC concentrations but restricted to the locations and time periods of the AMS observations. Figure 6 compares these two simulated distributions. We found that simulated VOC concentrations at the AMS locations were broadly representative of the global simulated distribution of isoprene and monoterpenes, but are skewed to high VOC_A and low VOC_{BB} concentrations. For example, about 35% of the AMS observations are in locations where simulated VOC_A is between 200–500 pptv, whereas only about 10% of the continental grid squares

Aerosol mass spectrometer constraint on the global SOA budget

D. V. Spracklen et al.

[Title Page](#)

[Abstract](#)

[Introduction](#)

[Conclusions](#)

[References](#)

[Tables](#)

[Figures](#)

◀

▶

◀

▶

[Back](#)

[Close](#)

[Full Screen / Esc](#)

[Printer-friendly Version](#)

[Interactive Discussion](#)



have this concentration in the global model. This skew to polluted locations is because the majority of AMS observations have taken place in the relatively polluted NH mid-latitudes. This analysis can be used to suggest where future AMS observations should be prioritised. Locations with $\text{VOC}_A < 20 \text{ pptv}$ and high isoprene, monoterpene or VOC_{BB} in Fig. 1 (e.g. many locations in the tropical Southern Hemisphere, such as the Amazon basin, Central Africa, Northern Australia) would diversify the observation dataset most effectively.

To remove this sampling bias from the AMS dataset we weighted each AMS observation by the ratio of the frequency of occurrence in the probability distribution for that location and the frequency of occurrence in the global probability distribution. We did this cumulatively for each VOC. This particularly increased the weight of AMS observations at low VOC_A concentrations and resulted in the most heavily weighted observations being central Amazon (AMAZE, weighted by a factor 12) and coastal Chile (VOCALS, weighted by a factor 7).

We reran our linear equations, but now using the weighting according to the above analysis. Figure 5c and d show a repeat of the fits shown in Fig. 5a and b but using the weighted dataset. The optimised SOA source using these weighted observations was $140 \pm 90 \text{ Tg (SOA) } \text{a}^{-1}$, consisting of $7 \pm 7 \text{ Tg (SOA) } \text{a}^{-1}$ from isoprene, $6 \pm 6 \text{ Tg (SOA) } \text{a}^{-1}$ from monoterpene, $3 \pm 4 \text{ Tg (SOA) } \text{a}^{-1}$ from biomass burning, $100 \pm 60 \text{ Tg (SOA) } \text{a}^{-1}$ anthropogenically controlled SOA and $23 \pm 15 \text{ Tg (SOA) } \text{a}^{-1}$ from aged POA. Weighting the observations therefore does not greatly impact the total SOA source calculated or the source from anthropogenic pollution, biomass burning or from aged POA, but increases the SOA from biogenic sources from 2 to $13 \text{ Tg (SOA) } \text{a}^{-1}$. We also optimised the SOA sources against both OA and OOA. As before this did not change the optimised sources greatly: optimised sources were $145 \pm 90 \text{ Tg (SOA) } \text{a}^{-1}$ consisting of $6 \pm 6 \text{ Tg (SOA) } \text{a}^{-1}$ from isoprene, $6 \pm 6 \text{ Tg (SOA) } \text{a}^{-1}$ from monoterpene, $4 \pm 5 \text{ Tg (SOA) } \text{a}^{-1}$ from biomass burning, $100 \pm 65 \text{ Tg (SOA) } \text{a}^{-1}$ anthropogenically controlled SOA and $31 \pm 25 \text{ Tg (SOA) } \text{a}^{-1}$ from aged POA.

Aerosol mass spectrometer constraint on the global SOA budget

D. V. Spracklen et al.

[Title Page](#)

[Abstract](#)

[Introduction](#)

[Conclusions](#)

[References](#)

[Tables](#)

[Figures](#)

◀

▶

[Back](#)

[Close](#)

[Full Screen / Esc](#)

[Printer-friendly Version](#)

[Interactive Discussion](#)



3.4 Discussion of the optimisation methods

Our different methods of SOA source optimisation described in Sects. 3.2 and 3.3 (weighted or unweighted AMS dataset, optimising against only OOA or both OA and OOA observations) changes the total optimised SOA source by less than 10% (range:

- 5 130–145 Tg (SOA) a^{-1}). The anthropogenically controlled SOA source is also very robust, with the different approaches changing the optimised source by less than 5% (range: 95–100 Tg (SOA) a^{-1}). The biomass burning source is uncertain but always relatively small in our analysis (range: 2–4 Tg (SOA) a^{-1}). Both the biogenic SOA (monoterpenes and isoprene, range: 2–13 Tg (SOA) a^{-1}) and aged POA sources (23–
10 31 Tg (SOA) a^{-1}) are less well constrained due to the limited number of observations
15 that have been made in air that is both heavily impacted by these sources and remote enough from anthropogenic pollution so as the signal from these smaller sources is not swamped. For the rest of the work we use the optimised SOA source constrained against OOA using the weighted AMS dataset as we believe that this is likely to give the strongest constraint. However, as we have shown our choice of method does not greatly impact our results.

3.5 Optimised SOA sources in the global model

We reran the global model using our optimised SOA sources (simulation 34, Table 2). With these optimised sources GLOMAP better simulates both AMS-observed

- 20 OA (NMB = −12%, NME = 59%, r^2 = 0.31) and OOA (NMB = −11%, NME = 53%, r^2 = 0.23) compared to the standard model (simulation 1, OA: NMB = −68%, NME = 74%, r^2 = 0.27; OOA: NMB = −85%, NME = 87%, r^2 = 0.00).

We also used observations from the IMPROVE network as an independent check to test the optimised sources in the global model (Fig. 7). We compared against year 25 2000 monthly mean organic carbon observations from IMPROVE. The baseline model underpredicts organic carbon observed by IMPROVE (NMB = −66%, NME = 68%) as has been shown previously (Mann et al., 2010). Increasing the SOA yield from biogenic

[Title Page](#)[Abstract](#)[Introduction](#)[Conclusions](#)[References](#)[Tables](#)[Figures](#)[◀](#)[▶](#)[Back](#)[Close](#)[Full Screen / Esc](#)[Printer-friendly Version](#)[Interactive Discussion](#)

VOCs reduces the model bias but does little to improve the model error ($\text{NMB} = -58\%$, $\text{NME} = 63\%$; $\text{NMB} = 32\%$, $\text{NME} = 95\%$; Fig. 7b and c). The model with optimised SOA sources (simulation 34, Fig. 7d) has smaller model error and bias ($\text{NMB} = -7\%$, $\text{NME} = 51\%$). The model has a slightly smaller bias ($\text{NMB} = 1\%$) when compared against the 2000–2004 average monthly mean IMPROVE observations. Interannual variability in wildfires which has been shown to dominate the interannual variability in OC aerosol concentrations over the United States (Spracklen et al., 2007) may explain the slightly low bias when compared against year 2000 observations.

Figure 8 shows the global distribution of simulated surface SOA concentrations. Annual mean surface SOA concentrations greater than $4 \mu\text{g m}^{-3}$ are simulated over the SE United States, India, China and the biomass burning regions of western and central Africa. The maximum contribution from biogenic sources is $1\text{--}2 \mu\text{g m}^{-3}$ over parts of the Amazon and Congo. Biomass burning results in SOA concentrations of $2 \mu\text{g m}^{-3}$ over Africa due to production from biomass burning VOCs and from POA to SOA conversion. Anthropogenically controlled SOA concentrations exceed $4 \mu\text{g m}^{-3}$ in the SE United States, India and China.

Our optimised SOA source ($140 \pm 90 \text{Tg(SOA a}^{-1}\text{)}$ is about a factor 2 greater than the upper end of bottom-up estimates used in global model studies ($12\text{--}70 \text{Tg(SOA a}^{-1}\text{)$, Kanakidou et al., 2005) and at the lower end of recent top-down estimates ($280\text{--}1820 \text{Tg(SOA a}^{-1}\text{)$: Goldstein and Galbally, 2007; $50\text{--}420 \text{Tg(SOA a}^{-1}\text{)$, Hallquist et al., 2009). Our estimated SOA source from ageing of POA ($23 \pm 15 \text{Tg(SOA a}^{-1}\text{)$) is within the range ($10\text{--}66 \text{Tg(SOA a}^{-1}\text{)$) from Hallquist et al. (2009). Our optimised anthropogenically controlled SOA source ($100 \pm 60 \text{Tg(SOA a}^{-1}\text{)$) is above the upper end of the range ($4\text{--}24 \text{Tg(SOA a}^{-1}\text{)$) suggested by Hallquist et al. (2009) and also above the estimate of $13.5 \text{Tg(SOA a}^{-1}\text{)$ from de Gouw and Jimenez (2009). Below we use radiocarbon observations to further investigate the origin of this source. Our optimised biogenic SOA source ($13 \pm 9 \text{Tg(SOA a}^{-1}\text{)$) is at the lower end of previous estimates, being 1–2 orders-of-magnitude lower than the range of estimates from Goldstein and Galbally (2007)

Aerosol mass spectrometer constraint on the global SOA budget

D. V. Spracklen et al.

[Title Page](#)

[Abstract](#)

[Introduction](#)

[Conclusions](#)

[References](#)

[Tables](#)

[Figures](#)

◀

▶

◀

▶

[Back](#)

[Close](#)

[Full Screen / Esc](#)

[Printer-friendly Version](#)

[Interactive Discussion](#)



although within the very broad range (0–360 Tg (SOA) a^{-1}) from Hallquist et al. (2009). Assuming the biogenic VOC emissions we assume are correct, our biogenic SOA source of 13 Tg (SOA) a^{-1} implies an SOA yield from isoprene plus monoterpenes of ~2%.

Our total simulated burden of SOA is 1.84 ± 1.14 Tg SOA, more than a factor 2 greater than recent global model studies (e.g., 0.81 Tg SOA; Henze et al., 2008). We estimate the uncertainty in our SOA burden by running the global model with the lower and upper estimate of our SOA sources.

Figure 9 shows the fractional contribution of biogenic, biomass and anthropogenically controlled sources to total simulated SOA concentrations. The substantial contribution of anthropogenically controlled SOA (100 Tg (SOA) a^{-1} , 70% of total SOA source) is not consistent with current understanding of SOA formation from anthropogenic VOCs. Previous global model studies, those including more recent parameterisations, suggest that anthropogenic VOCs contribute less than 10 Tg (SOA) a^{-1} (e.g., Tsigaridis et al., 2006; Heald et al., 2008; Henze et al., 2008, Farina et al., 2010). Our optimised SOA source would require an average SOA yield of 79% from anthropogenic VOCs. Whilst such high yields have been observed in laboratory studies under certain conditions for species such as for toluene and benzene (Ng et al., 2007; Hildebrandt et al., 2009), this yield is substantially larger than expected for the majority of anthropogenic VOCs. Pye and Seinfeld (2010) predict that primary anthropogenic emissions of S/IVOCs can produce substantial quantities of SOA. The EDGAR inventory, from which we obtain global emissions of anthropogenic VOCs, does not include emissions of S/IVOCs and this could potentially explain some of our anthropogenically controlled SOA. To further examine the fraction of SOA that can be attributed to anthropogenic VOCs, in the next section we analyse radiocarbon data.

Aerosol mass spectrometer constraint on the global SOA budget

D. V. Spracklen et al.

[Title Page](#)

[Abstract](#)

[Introduction](#)

[Conclusions](#)

[References](#)

[Tables](#)

[Figures](#)

◀

▶

[Back](#)

[Close](#)

[Full Screen / Esc](#)

[Printer-friendly Version](#)

[Interactive Discussion](#)



3.6 Radiocarbon observations

We used radiocarbon data to test our optimised source-specific SOA sources. Measurements of the radiocarbon ^{14}C : ^{12}C ratio in ambient aerosol have been used to estimate the fraction of total carbon aerosol that is modern (non-fossil). Such analysis shows that a large fraction (typically 80–100%) of OA in rural regions of the SE United States is non-fossil (Bench et al., 2007; Weber et al., 2007; Ding et al., 2008).

We supplemented the ^{14}C dataset compiled by Hodzic et al. (2010b) with additional observations from Bench et al. (2007). Mass concentrations of total carbon aerosol reported in the combined ^{14}C dataset (mean $7.9 \mu\text{g C m}^{-3}$, median $4.9 \mu\text{g C m}^{-3}$) are greater than total carbon aerosol observed by IMPROVE (year 2000 mean $1.65 \mu\text{g C m}^{-3}$, median $1.22 \mu\text{g C m}^{-3}$) or OA observed by AMS (mean $2.1 \mu\text{g C m}^{-3}$, median $1.5 \mu\text{g C m}^{-3}$). This may be due to the ^{14}C dataset being biased to locations and/or periods of high OC concentrations, perhaps due to the need for high amounts of OA for successful ^{14}C analysis, especially with older instrumentation (Schichtel et al., 2008). Figure 10a shows a comparison between simulated and observed total carbon aerosol. Both the standard (simulation 1) and optimised model (simulation 34) underpredicted total carbon aerosol reported by this database (NMB = -85% and NMB = -72% respectively). Model performance was worst at sites classified as “urban” or “valley”, likely because the coarse resolution of the global model is unable to resolve urban scale pollution. When we restricted analysis to sites that were classified as “remote”, the standard model underpredicted total carbon aerosol mass (NMB = -58%) whereas the optimised model was in good agreement (NMB = -4%). We therefore restricted our comparison of ^{14}C data to the remote sites where the optimised model was able to well simulate total carbon mass concentrations.

The ^{14}C database has a mean non-fossil fraction of 65% across all sites and 84% when restricted to sites that are classified as remote. We note that some of the values in the dataset may overestimate non-fossil carbon by 0–10%, depending on the mix of non-fossil sources, due to not accounting for the higher ^{14}C from wood combustion

Aerosol mass spectrometer constraint on the global SOA budget

D. V. Spracklen et al.

[Title Page](#)

[Abstract](#)

[Introduction](#)

[Conclusions](#)

[References](#)

[Tables](#)

[Figures](#)

◀

▶

[Back](#)

[Close](#)

[Full Screen / Esc](#)

[Printer-friendly Version](#)

[Interactive Discussion](#)



(Szidat et al., 2009). However, this uncertainty is small compared to the discrepancy between observed and simulated non-fossil carbon that we report below. We calculated the non-fossil fraction simulated using our optimised SOA sources. We assumed that 20% of anthropogenically controlled SOA is non-fossil, as our best estimate for urban pollution sources (Hildemann et al., 1994; Hodzic et al., 2010b). With this assumption we simulated an average non-fossil fraction at remote sites of 25% (NMB = -71%), underpredicting non-fossil carbon (NMB = -67%) and overpredicting fossil-carbon (NMB = 271%) (Fig. 10b–d).

We then varied the fraction of optimised anthropogenically controlled SOA source that would need to be non-fossil to match the ^{14}C data at remote sites. When we assumed that 93% of anthropogenically controlled SOA was non-fossil the model best matched both fossil (NMB = 0.9%) and non-fossil carbon (NMB = -5%). With this assumption the model predicted a mean non-fossil fraction of 73% at remote sites which was close to the observed value (NMB = -13%).

We use this analysis to further classify our “anthropogenically controlled” SOA. Our analysis suggests a maximum of 10% ($\sim 10 \text{ Tg (SOA) a}^{-1}$) of the anthropogenically controlled SOA is from anthropogenic VOCs. In the rest of the paper we define the 10% of the “anthropogenically controlled” SOA that appears to be arising from anthropogenic VOCs as Urban SOA, in line with de Gouw and Jimenez (2009). Our estimate is broadly consistent with previous estimates: 6–34 Tg (SOA) a^{-1} (Hallquist et al., 2009) and 2–12 Tg (SOA) a^{-1} (Henze et al., 2008) from anthropogenic VOCs and with the urban SOA source of $13.5 \text{ Tg (SOA) a}^{-1}$ estimated by de Gouw and Jimenez (2009). The majority of our anthropogenically controlled SOA source ($\sim 90\%$, $90 \text{ Tg (SOA) a}^{-1}$) is therefore likely to come from sources other than anthropogenic VOCs. It is possible that a fraction of this source could arise from an underestimated impact of biomass burning in the mid latitudes, however this appears unlikely to explain a significant fraction of the source. Previous studies have suggested a role for anthropogenic pollution in the enhancement of SOA formation from biogenic VOCs (de Gouw et al., 2005; Weber et al., 2007; Goldstein et al., 2009), and the recent modelling study of Carlton et

Aerosol mass spectrometer constraint on the global SOA budget

D. V. Spracklen et al.

[Title Page](#)

[Abstract](#)

[Introduction](#)

[Conclusions](#)

[References](#)

[Tables](#)

[Figures](#)

◀

▶

[Back](#)

[Close](#)

[Full Screen / Esc](#)

[Printer-friendly Version](#)

[Interactive Discussion](#)



al. (2010) suggests that pollution enhances biogenic SOA formation over the US by a factor of 2. Our analysis suggests a substantially larger enhancement. Additionally, much of the effect that causes the enhancement in the Carlton et al. study (such as higher oxidants in polluted regions) are already included in our standard model.

5 Therefore if a substantial fraction of our inferred “anthropogenically controlled” SOA is arising from biogenic VOC, the enhancement of SOA yield due to pollution is almost an order-of-magnitude greater than is currently understood. We term this SOA source as “anthropogenically controlled” biogenic SOA (AC-BSOA). If we sum the “biogenic” plus AC-BSOA source, the net SOA yield from monoterpenes plus isoprene is ~16%.

10 Figure 11 shows the estimated zonal distribution of our optimised OA sources compared to those estimated by de Gouw and Jimenez (2010). Our total OA source (both primary and secondary) is $164 \text{ Tg(OA)} \text{ a}^{-1}$, with a total SOA source of $140 \text{ Tg(SOA)} \text{ a}^{-1}$ (including oxidation of POA to SOA) or $117 \text{ Tg(SOA)} \text{ a}^{-1}$ (excluding oxidation of POA). This compares to a total SOA source of $45 \text{ Tg(SOA)} \text{ a}^{-1}$ estimated

15 by de Gouw and Jimenez (2009). Our total SOA source is larger due to the large source of SOA we infer from anthropogenic enhancement of biogenic SOA that was not included in de Gouw and Jimenez (2009). Our estimated urban SOA source is similar to that of de Gouw and Jimenez (2009). We estimate a substantial source of SOA from oxidation of POA ($23 \pm 15 \text{ Tg(SOA)} \text{ a}^{-1}$), that is not shown in Fig. 11 as it is included in the POA source.

20 3.7 Estimation of aerosol forcing due to anthropogenically controlled SOA

We estimated the aerosol direct effect (ADE) and the cloud albedo aerosol indirect effect (AIE) due to the presence of the anthropogenically controlled SOA. We did this through comparing model runs with and without our optimised anthropogenically controlled SOA source. We estimate an uncertainty in the radiative effect of the anthropogenically controlled SOA source using the upper ($160 \text{ Tg(SOA)} \text{ a}^{-1}$) and lower ($40 \text{ Tg(SOA)} \text{ a}^{-1}$) limit of our source estimate.

Aerosol mass spectrometer constraint on the global SOA budget

D. V. Spracklen et al.

[Title Page](#)

[Abstract](#)

[Introduction](#)

[Conclusions](#)

[References](#)

[Tables](#)

[Figures](#)

◀

▶

◀

▶

[Back](#)

[Close](#)

[Full Screen / Esc](#)

[Printer-friendly Version](#)

[Interactive Discussion](#)



To estimate the ADE we used the anthropogenically controlled SOA burden simulated by GLOMAP along with the AeroCom multi-model mean OA burden (0.66 Tg) and multi-model mean ADE (-0.13 Wm^{-2}). The GLOMAP simulated burden of anthropogenically controlled SOA ($1.3 \pm 0.8 \text{ Tg}$) results in an estimated ADE of $-0.26 \pm 0.15 \text{ Wm}^{-2}$. This estimation assumes that the optical properties of the anthropogenic SOA are identical to that of OA within the AeroCom models. More sophisticated estimates of the ADE from anthropogenically-controlled SOA are now required.

To calculate the AIE we first calculated the cloud drop number concentrations (CDNC) with (perturbed) and without (baseline) anthropogenically controlled SOA. Both the baseline and perturbed runs included all other aerosol sources treated in this study. We calculated CDNC using the simulated aerosol size distribution and a mechanistic parameterization of cloud drop formation (Nenes and Seinfeld, 2003). We have shown previously that this method produces realistic CDNC (Merikanto et al., 2010).

We calculated cloud albedo using the off-line version of the Edwards and Slingo (1996) radiative transfer model together with monthly mean climatological cloud fields and surface albedo (averaged over the period 1983–2005) from the International Satellite Cloud Climatology (ISCCP) (Rossow and Schiffer, 1999). The model uses 9 bands in the longwave and 6 bands in the shortwave and a delta-Eddington 2 stream scattering solver at all wavelengths. In our climatology, the clouds were added to three unique vertical levels, corresponding to low and middle and high clouds. Water vapour, temperature and ozone data are based on European Centre for Medium-Range Weather Forecasting reanalysis data (see Rap et al., 2010 for details). For the unperturbed and perturbed runs, cloud effective drop radius r_e (in μm) for low and mid level water clouds was calculated from the GLOMAP CDNC (in cm^{-3}) and ISCCP derived liquid water paths (LWP, in g m^{-2}), using the Bower et al. (1994) parameterisation, namely:

$$r_e = 100 \times [\text{LWP}/(\Delta z) \times 3/(4\pi \times \text{CDNC})]^{1/3},$$

Aerosol mass spectrometer constraint on the global SOA budget

D. V. Spracklen et al.

[Title Page](#)

[Abstract](#)

[Introduction](#)

[Conclusions](#)

[References](#)

[Tables](#)

[Figures](#)

◀

▶

[Back](#)

[Close](#)

[Full Screen / Esc](#)

[Printer-friendly Version](#)

[Interactive Discussion](#)



where Δz is the cloud thickness, which in our climatology is roughly 1400 m and 2900 m for low and middle clouds, respectively. Only water clouds were modified.

The cloud albedo AIE at the top of the atmosphere was then calculated by comparing the cloud albedo calculated with anthropogenically controlled SOA compared to the cloud albedo calculated without anthropogenically controlled SOA. Figure 12 shows the AIE due to our anthropogenically controlled SOA source. We calculate a global annual mean AIE of $-0.6^{+0.24}_{-0.14} \text{ Wm}^{-2}$. Our calculated AIE is substantial compared with the IPCC value of $-0.7 \pm 0.4 \text{ Wm}^{-2}$, which does not include SOA. Future work is now needed to explore uncertainties in the contribution of this anthropogenically controlled SOA to particle growth rates and the interaction with BL particle formation (Spracklen et al., 2008a) both of which may greatly impact the contribution to the formation of CCN and the AIE.

4 Conclusions

We have used a 3-D chemical transport model and a global dataset of organic aerosol (OA) observed by the AMS to produce new top-down constraints on the secondary organic aerosol (SOA) budget. Our optimised model has a global SOA source of $140 \pm 90 \text{ Tg (SOA) a}^{-1}$ which is a factor of two greater than bottom-up estimates but at the lower end of previous top-down studies (Fig. 14). Our optimised SOA sources also improved comparison with OA observations over the United States made by IMPROVE. The total OA source (including primary organic aerosol) in our study is $164 \pm 90 \text{ Tg (OA) a}^{-1}$. Our estimate is similar to a recent top-down estimate of the OA budget using satellite observations of aerosol optical depth and a global model (Heald et al., 2010) which suggested an OA source of $300 \pm 240 \text{ Tg (OA) a}^{-1}$ (assuming a 2:1 OA:OC conversion).

We resolved the SOA budget into 4 different sources with $100 \pm 60 \text{ Tg (SOA) a}^{-1}$ from anthropogenically controlled sources, $13 \pm 8 \text{ Tg (SOA) a}^{-1}$ from biogenic sources, $3 \pm 3 \text{ Tg (SOA) a}^{-1}$ from biomass burning and $23 \pm 15 \text{ Tg (SOA) a}^{-1}$ from conversion of

[Title Page](#)[Abstract](#)[Introduction](#)[Conclusions](#)[References](#)[Tables](#)[Figures](#)[◀](#)[▶](#)[◀](#)[▶](#)[Back](#)[Close](#)[Full Screen / Esc](#)[Printer-friendly Version](#)[Interactive Discussion](#)

POA (mostly from biomass burning sources). We used ^{14}C (radiocarbon) observations made in remote locations to characterise the anthropogenically controlled SOA source. Assuming that the anthropogenically controlled SOA source is largely from anthropogenic VOCs is inconsistent with measured fractions of non-fossil carbon in OA in remote regions. To match the non-fossil fraction calculated from ^{14}C observations we estimate that a maximum of $\sim 10 \text{ Tg} (\text{SOA}) \text{ a}^{-1}$ can be formed directly from anthropogenic VOCs. We ascribe the remaining $90 \text{ Tg} (\text{SOA}) \text{ a}^{-1}$ to anthropogenic pollution enhancement of SOA formation from biogenic VOCs as suggested in previous studies (e.g., de Gouw et al., 2005; Weber et al., 2007). The majority of ^{14}C observations have been made in urban or sub-urban locations and we suggest that additional observations are required in locations remote from anthropogenic pollution. This anthropogenically controlled SOA source that we infer results in a larger SOA source in the Northern Hemisphere mid-latitudes than in previous studies.

The magnitude of the potential enhancement by pollution of SOA formation from biogenic VOCs appears to be almost an order-of-magnitude larger than with currently proposed mechanisms. Carlton et al. (2010) use the terms “controllable” and “non-controllable” to classify SOA from biogenic VOCs, and suggests that about $1/2$ of the SOA from biogenic VOCs is controllable. Our work suggests that this fraction of controllable biogenic-VOC may be even larger, but says nothing about the mechanism and therefore gives little guidance to policy efforts that might be aimed at reducing SOA. Future process studies in the field and the laboratory need to investigate the mechanisms by which this potential enhancement may occur. We estimate that this anthropogenically controlled SOA results in an aerosol direct effect of $-0.26 \pm 0.15 \text{ Wm}^{-2}$ and a cloud albedo aerosol indirect effect of $-0.6_{-0.14}^{+0.24} \text{ Wm}^{-2}$. Our calculated cloud albedo radiative effect is substantial compared to the aerosol indirect effect from all anthropogenic aerosol of $-0.7 \pm 0.4 \text{ Wm}^{-2}$ calculated by the IPCC (Forster et al., 2007), but which did not include SOA.

The AMS database used in this analysis is spatially limited, lacks information on the seasonal cycle at most locations and has very limited information on the vertical

Aerosol mass spectrometer constraint on the global SOA budget

D. V. Spracklen et al.

[Title Page](#)

[Abstract](#)

[Introduction](#)

[Conclusions](#)

[References](#)

[Tables](#)

[Figures](#)



[Back](#)

[Close](#)

[Full Screen / Esc](#)

[Printer-friendly Version](#)

[Interactive Discussion](#)

- OA profile. We have shown that the location of observations in the database is representative of biogenic VOC concentrations over land, but it is biased to regions of higher anthropogenic pollution. We attempt to account for this bias in sampling by differentially weighting the AMS observations and find that it does not greatly alter our estimated SOA sources. To enable tighter constraints from analysis with the methods presented here, additional OA observations are required in locations that have small influence from anthropogenic pollution and high influence from biogenic and/or biomass burning sources, such as in the tropics, particularly Amazonia, Central Africa, Northern Australia, the Southern Hemisphere and remote boreal forest locations.
- 5
- 10 Acknowledgements. We acknowledge the support of the following grants: UK Natural Environmental Research Council (NERC) grant (NE/G015015/1), US DOE (BER, ASR Program) DEFG0208ER64627, NOAA NA08OAR4310565, US NSF ATM-0449815 (CAREER) and ATM-0919189, and US EPA R833747.

References

- 15 Aiken, A. C., DeCarlo, P. F., Kroll, J. H., Worsnop, D. R., Huffman, J. A., Docherty, K. S., Ulbrich, I. M., Mohr, C., Kimmel, J. R., Sueper, D., Sun, Y., Zhang, Q., Trimborn, A., Northway, M., Ziemann, P. J., Canagaratna, M. R., Onasch, T. B., Alfarra, M. R., Prevot, A. S. H., Dommen, J., Duplissy, J., Metzger, A., Baltensperger, U., and Jimenez, J. L.: O/C and OM/OC ratios of primary, secondary and ambient organic aerosols with high-resolution time-of-flight aerosol mass spectrometry, Environ. Sci. Technol., 42(12), 4478–4485, doi:10.1021/es703009q, 2008.
- 20
- 25 Aiken, A. C., Salcedo, D., Cubison, M. J., Huffman, J. A., DeCarlo, P. F., Ulbrich, I. M., Docherty, K. S., Sueper, D., Kimmel, J. R., Worsnop, D. R., Trimborn, A., Northway, M., Stone, E. A., Schauer, J. J., Volkamer, R. M., Fortner, E., de Foy, B., Wang, J., Laskin, A., Shutthanandan, V., Zheng, J., Zhang, R., Gaffney, J., Marley, N. A., Paredes-Miranda, G., Arnott, W. P., Molina, L. T., Sosa, G., and Jimenez, J. L.: Mexico City aerosol analysis during MILAGRO using high resolution aerosol mass spectrometry at the urban supersite (T0) – Part 1: Fine particle composition and organic source apportionment, Atmos. Chem. Phys., 9, 6633–6653, doi:10.5194/acp-9-6633-2009, 2009.

[Title Page](#)[Abstract](#)[Introduction](#)[Conclusions](#)[References](#)[Tables](#)[Figures](#)[Back](#)[Close](#)[Full Screen / Esc](#)[Printer-friendly Version](#)[Interactive Discussion](#)

- Allan, J. D., Bower, K. N., Coe, H., Boudries, H., Jayne, J. T., Canagaratna, M. R., Millet, D. B., Goldstein, A. H., Quinn, P. K., Weber, R. J., and Worsnop, D. R.: Submicron aerosol composition at Trinidad Head, California, during ITCT 2K2: Its relationship with gas phase volatile organic carbon and assessment of instrument performance, *J. Geophys. Res.*, 109(D23), D23S24, doi:10.1029/2003JD004208, 2004.
- Arnold, S. R., Chipperfield, M. P., and Blitz, M. A.: A three-dimensional model study of the effect of new temperature-dependent quantum yields for acetone photolysis, *J. Geophys. Res.*, 110, D22305, doi:10.1029/2005JD005998, 2005.
- Arnold, S. R., Spracklen, D. V., Williams, J., Yassaa, N., Sciare, J., Bonsang, B., Gros, V., Peeken, I., Lewis, A. C., Alvain, S., and Moulin, C.: Evaluation of the global oceanic isoprene source and its impacts on marine organic carbon aerosol, *Atmos. Chem. Phys.*, 9, 1253–1262, doi:10.5194/acp-9-1253-2009, 2009.
- Bench, G., Fallon, S., Schichtel, B., Malm, W., and McDade, C.: Relative contributions of fossil and contemporary carbon sources to PM 2.5 aerosols at nine Interagency Monitoring for Protection of Visual Environments (IMPROVE) network sites, *J. Geophys. Res.*, 112, D10205, doi:10.1029/2006JD007708, 2007.
- Canagaratna, M. R., Jayne, J. T., Jimenez, J. L., Allan, J. D., Alfarra, M. R., Zhang, Q., Onasch, T. B., Drewnick, F., Coe, H., Middlebrook, A., Delia, A., Williams, L. R., Trimborn, A. M., Northway, M. J., DeCarlo, P. F., Kolb, C. E., Davidovits, P., and Worsnop, D. R.: Chemical and microphysical characterization of ambient aerosols with the aerodyne mass spectrometer, *Mass Spectrom. Rev.*, 26(2), 185–222, 2007.
- Capes, G., Johnson, B., McFiggans, G., Williams, P. I., Haywood, J., and Coe, H.: Aging of biomass burning aerosols West Africa: Aircraft measurements of chemical composition, microphysical properties, and emission ratios, *J. Geophys. Res.*, 113, D00C15, doi:10.1029/2008JD009845, 2008.
- Capes, G., Murphy, J. G., Reeves, C. E., McQuaid, J. B., Hamilton, J. F., Hopkins, J. R., Crosier, J., Williams, P. I., and Coe, H.: Secondary organic aerosol from biogenic VOCs over West Africa during AMMA, *Atmos. Chem. Phys.*, 9, 3841–3850, doi:10.5194/acp-9-3841-2009, 2009.
- Cappa, C. D. and Jimenez, J. L.: Quantitative estimates of the volatility of ambient organic aerosol, *Atmos. Chem. Phys.*, 10, 5409–5424, doi:10.5194/acp-10-5409-2010, 2010.
- Cappa, C. D. and Wilson, K. R.: Evolution of organic aerosol mass spectra upon heating: implications for OA phase and partitioning behavior, *Atmos. Chem. Phys. Discuss.*, 10, 28431–

Aerosol mass spectrometer constraint on the global SOA budget

D. V. Spracklen et al.

[Title Page](#)[Abstract](#)[Introduction](#)[Conclusions](#)[References](#)[Tables](#)[Figures](#)[Back](#)[Close](#)[Full Screen / Esc](#)[Printer-friendly Version](#)[Interactive Discussion](#)

- Carlton, A. G., Pinder, R. W., Bhave, P. V., and Pouliot, G. A.: To what extent can biogenic SOA be controlled, *Environ. Sci. Technol.*, 44, 3376–3380, doi:10.1021/es903506b, 2010.
- Chan, A. W. H., Chan, M. N., Surratt, J. D., Chhabra, P. S., Loza, C. L., Crounse, J. D., Yee, L. D., Flagan, R. C., Wennberg, P. O., and Seinfeld, J. H.: Role of aldehyde chemistry and NO_x concentrations in secondary organic aerosol formation, *Atmos. Chem. Phys.*, 10, 7169–7188, doi:10.5194/acp-10-7169-2010, 2010.
- Chen, Q., Farmer, D. K., Schneider, J., Zorn, S. R., Heald, C. L., Karl, T. G., Guenther, A., Allan, J. D., Robinson, N., Coe, H., Kimmel, J. R., Pauliquevis, T., Borrmann, S., Pöschl, U., Andreae, M. O., Artaxo, P., Jimenez, J. L., and Martin, S. T.: Mass spectral characterization of submicron biogenic organic particles in the Amazon Basin, *Geophys. Res. Lett.*, 36, L20806, doi:10.1029/2009GL039880, 2009.
- Chipperfield, M. P.: New version of the TOMCAT/SLIMCAT off-line chemical transport model: Intercomparison of stratospheric tracer experiments, *Q. J. Roy. Meteorol. Soc.*, 132(617B), 1179–1203, 2006.
- Cottrell, L. D., Griffin, R. J., Jimenez, J. L., Zhang, Q., Ulbrich, I., Ziembka, L. D., Beckman, P. J., Sive, B. C., and Talbot, R. W.: Submicron particles at Thompson Farm during ICARTT measured using aerosol mass spectrometry, *J. Geophys. Res.*, 113, D08212, doi:10.1029/2007JD009192, 2008.
- DeCarlo, P. F., Ulbrich, I. M., Crounse, J., de Foy, B., Dunlea, E. J., Aiken, A. C., Knapp, D., Weinheimer, A. J., Campos, T., Wennberg, P. O., and Jimenez, J. L.: Investigation of the sources and processing of organic aerosol over the Central Mexican Plateau from aircraft measurements during MILAGRO, *Atmos. Chem. Phys.*, 10, 5257–5280, doi:10.5194/acp-10-5257-2010, 2010.
- de Gouw, J. A., Middlebrook, A. M., Warneke, C., Goldan, P. D., Kuster, W. C., Roberts, J. M., Fehsenfeld, F. C., Worsnop, D. R., Canagaratna, M. R., Pszenny, A. A. P., Keene, W. C., Marchewka, M., Bertman, S. B., and Bates, T. S.: Budget of organic carbon in a polluted atmosphere: Results from the New England Air Quality Study in 2002, *J. Geophys. Res.*, 110, D16305, doi:10.1029/2004JD005623, 2005.
- de Gouw, J. A., Brock, C. A., Atlas, E. L., Bates, T. S., Fehsenfeld, F. C., Goldan, P. D., Holloway, J. S., Kuster, W. C., Lerner, B. M., Matthew, B. M., Middlebrook, A. M., Onasch, T. B., Peltier, R. E., Quinn, P. K., Senff, C. J., Stohl, A., Sullivan, A. P., Trainer, M., Warneke, C., Weber, R. J., and Williams, E. J.: Sources of particulate matter in the northeastern United States in

Aerosol mass spectrometer constraint on the global SOA budget

D. V. Spracklen et al.

[Title Page](#)

[Abstract](#)

[Introduction](#)

[Conclusions](#)

[References](#)

[Tables](#)

[Figures](#)

◀

▶

◀

▶

[Back](#)

[Close](#)

[Full Screen / Esc](#)

[Printer-friendly Version](#)

[Interactive Discussion](#)



Aerosol mass spectrometer constraint on the global SOA budget

D. V. Spracklen et al.

[Title Page](#)

[Abstract](#)

[Introduction](#)

[Conclusions](#)

[References](#)

[Tables](#)

[Figures](#)

◀

▶

[Back](#)

[Close](#)

[Full Screen / Esc](#)

[Printer-friendly Version](#)

[Interactive Discussion](#)



Aerosol mass spectrometer constraint on the global SOA budget

D. V. Spracklen et al.

[Title Page](#)

[Abstract](#)

[Introduction](#)

[Conclusions](#)

[References](#)

[Tables](#)

[Figures](#)



[Back](#)

[Close](#)

[Full Screen / Esc](#)

[Printer-friendly Version](#)

[Interactive Discussion](#)



Aerosol mass spectrometer constraint on the global SOA budget

D. V. Spracklen et al.

- E., Atlas, E. L., de Gouw, J. A., Warneke, C., Holloway, J. S., Neuman, J. A., Flocke, F. M., and Seinfeld, J. H.: Concentrations and sources of organic carbon aerosols in the free troposphere over North America, *J. Geophys. Res.*, 111, D23S47, doi:10.1029/2006JD007705, 2006.
- 5 Heald, C. L., Henze, D. K., Horowitz, L. W., Feddema, J., Lamarque, J.-F., Guenther, A., Hess, P. G., Vitt, F., Seinfeld, J. H., Goldstein, A. H., and Fung, I.: Predicted change in global secondary organic aerosol concentrations in response to future climate, emissions, and land use change, *J. Geophys. Res.*, 113, D05211, doi:10.1029/2007JD009092, 2008.
- 10 Heald, C. L., Ridley, D.A., Kreidenweis, S. M., and Drury, E. E.: Satellite observations cap the atmospheric organic aerosol budget, *Geophys. Res. Lett.*, 37, L24808, doi:10.1029/2010GL045095, 2010.
- 15 Henze, D. K., Seinfeld, J. H., Ng, N. L., Kroll, J. H., Fu, T.-M., Jacob, D. J., and Heald, C. L.: Global modeling of secondary organic aerosol formation from aromatic hydrocarbons: high- vs. low-yield pathways, *Atmos. Chem. Phys.*, 8, 2405–2420, doi:10.5194/acp-8-2405-2008, 2008.
- 20 Hildebrandt, L., Donahue, N. M., and Pandis, S. N.: High formation of secondary organic aerosol from the photo-oxidation of toluene, *Atmos. Chem. Phys.*, 9, 2973–2986, doi:10.5194/acp-9-2973-2009, 2009.
- 25 Hildemann, L. M., Klinedinst, D. B., Klouda, G. A., Currie, L. A., and Cass, G. R.: Sources of Urban Contemporary Carbon Aerosol, *Environ. Sci. Technol.*, 28, 1565–1576, 1994.
- Hodzic, A., Jimenez, J. L., Madronich, S., Aiken, A. C., Bessagnet, B., Curci, G., Fast, J., Lamarque, J.-F., Onasch, T. B., Roux, G., Schauer, J. J., Stone, E. A., and Ulbrich, I. M.: Modeling organic aerosols during MILAGRO: importance of biogenic secondary organic aerosols, *Atmos. Chem. Phys.*, 9, 6949–6981, doi:10.5194/acp-9-6949-2009, 2009.
- 30 Hodzic, A., Jimenez, J. L., Madronich, S., Canagaratna, M. R., DeCarlo, P. F., Kleinman, L., and Fast, J.: Modeling organic aerosols in a megacity: potential contribution of semi-volatile and intermediate volatility primary organic compounds to secondary organic aerosol formation, *Atmos. Chem. Phys.*, 10, 5491–5514, doi:10.5194/acp-10-5491-2010, 2010a.
- Hodzic, A., Jimenez, J. L., Prévôt, A. S. H., Szidat, S., Fast, J. D., and Madronich, S.: Can 3-D models explain the observed fractions of fossil and non-fossil carbon in and near Mexico City?, *Atmos. Chem. Phys.*, 10, 10997–11016, doi:10.5194/acp-10-10997-2010, 2010b.
- Jang, M., Czoschke, N. M., Lee, S., and Kamens, R. M.: Heterogeneous Atmospheric Aerosol Production by Acid-Catalyzed Particle-Phase Reactions. *Science* 298, 814–817,

[Title Page](#)

[Abstract](#)

[Introduction](#)

[Conclusions](#)

[References](#)

[Tables](#)

[Figures](#)



[◀](#)

[▶](#)

[Back](#)

[Close](#)

[Full Screen / Esc](#)

[Printer-friendly Version](#)

[Interactive Discussion](#)



Aerosol mass spectrometer constraint on the global SOA budget

D. V. Spracklen et al.

- Jimenez, J. L., Canagaratna, M. R., Donahue, N. M., Prevot, A. S. H., Zhang, Q., Kroll, J. H., DeCarlo, P. F., Allan, J. D., Coe, H., Ng, N. L., Aiken, A. C., Docherty, K. S., Ulbrich, I. M., Grieshop, A. P., Robinson, A. L., Duplissy, J., Smith, J. D., Wilson, K. R., Lanz, V. A., Hueglin, C., Sun, Y. L., Tian, J., Laaksonen, A., Raatikainen, T., Rautiainen, J., Vaattovaara, P., Ehn, M., Kulmala, M., Tomlinson, J. M., Collins, D. R., Cubison, M. J., Dunlea, E. J., Huffman, J. A., Onasch, T. B., Alfarra, M. R., Williams, P. I., Bower, K., Kondo, Y., Schneider, J., Drewnick, F., Borrmann, S., Weimer, S., Demerjian, K., Salcedo, D., Cottrell, L., Griffin, R., Takami, A., Miyoshi, T., Hatakeyama, S., Shimono, A., Sun, J. Y., Zhang, Y. M., Dzepina, K., Kimmel, J. R., Sueper, D., Jayne, J. T., Herndon, S. C., Trimborn, A. M., Williams, L. R., Wood, E. C., Middlebrook, A. M., Kolb, C. E., Baltensperger, U., and Worsnop, D. R.: Evolution of organic aerosols in the atmosphere, *Science*, 326, 1525, doi:10.1126/science.1180353, 2009.
- Kanakidou, M., Seinfeld, J. H., Pandis, S. N., Barnes, I., Dentener, F. J., Facchini, M. C., Van Dingenen, R., Ervens, B., Nenes, A., Nielsen, C. J., Swietlicki, E., Putaud, J. P., Balkanski, Y., Fuzzi, S., Horth, J., Moortgat, G. K., Winterhalter, R., Myhre, C. E. L., Tsigaridis, K., Vignati, E., Stephanou, E. G., and Wilson, J.: Organic aerosol and global climate modelling: a review, *Atmos. Chem. Phys.*, 5, 1053–1123, doi:10.5194/acp-5-1053-2005, 2005.
- Kroll, J. H., Ng, N. L., Murphy, S. M., Flagan, R. C., and Seinfeld, J. H.: Secondary organic aerosol formation from isoprene photooxidation, *Environ. Sci. Technol.*, 40(6), 1869–1877, 2006.
- Lane, T. E., Donahue, N. M., and Pandis, S. N.: Simulating secondary organic aerosol formation using volatility basis-set approach in a chemical transport model, *Atmos. Environ.*, 42(32), 7439–7451, 2008.
- Lanz, V. A., Alfarra, M. R., Baltensperger, U., Buchmann, B., Hueglin, C., and Prévôt, A. S. H.: Source apportionment of submicron organic aerosols at an urban site by factor analytical modelling of aerosol mass spectra, *Atmos. Chem. Phys.*, 7, 1503–1522, doi:10.5194/acp-7-1503-2007, 2007.
- Malm, W. C., Schichtel, B. A., Pitchford, M. L., Ashbaugh, L. L., and Eldred, R. A.: Spatial and monthly trends in speciated fine particle concentration in the United States, *J. Geophys. Res.*, 109, D03306, doi:10.1029/2003JD003739, 2004.
- Manktelow, P. T., Mann, G. W., Carslaw, K. S., Spracklen, D. V., and Chipperfield, M. P.: Regional and global trends in sulfate aerosol since the 1980s, *Geophys. Res. Lett.*, 34, L14803, doi:10.1029/2006GL028668, 2007.

[Title Page](#)

[Abstract](#)

[Introduction](#)

[Conclusions](#)

[References](#)

[Tables](#)

[Figures](#)

◀

▶

[Back](#)

[Close](#)

[Full Screen / Esc](#)

[Printer-friendly Version](#)

[Interactive Discussion](#)



- Mann, G. W., Carslaw, K. S., Spracklen, D. V., Ridley, D. A., Manktelow, P. T., Chipperfield, M. P., Pickering, S. J., and Johnson, C. E.: Description and evaluation of GLOMAP-mode: a modal global aerosol microphysics model for the UKCA composition-climate model, *Geosci. Model Dev.*, 3, 519–551, doi:10.5194/gmd-3-519-2010, 2010.
- 5 Merikanto, J., Spracklen, D. V., Pringle, K. J., and Carslaw, K. S.: Effects of boundary layer particle formation on cloud droplet number and changes in cloud albedo from 1850 to 2000, *Atmos. Chem. Phys.*, 10, 695–705, doi:10.5194/acp-10-695-2010, 2010.
- Murphy, D. M., Cziczo, D. J., Froyd, K. D., Hudson, P. K., Matthew, B. M., Middlebrook, A. M., Peltier, R. E., Sullivan, A., Thomson, D. S., and Weber, R. J.: Single-particle mass spectrometry of tropospheric aerosol particles, *J. Geophys. Res.*, 111, D23S32, doi:10.1029/2006JD007340, 2006.
- 10 Nenes, A. and Seinfeld, J. H.: Parameterization of cloud droplet formation in global climate models, *J. Geophys. Res.*, 108, 4415, doi:10.1029/2002JD002911, 2003.
- Ng, N. L., Kroll, J. H., Chan, A. W. H., Chhabra, P. S., Flagan, R. C., and Seinfeld, J. H.: Secondary organic aerosol formation from m-xylene, toluene, and benzene, *Atmos. Chem. Phys.*, 7, 3909–3922, doi:10.5194/acp-7-3909-2007, 2007.
- 15 Ng, N. L., Kwan, A. J., Surratt, J. D., Chan, A. W. H., Chhabra, P. S., Sorooshian, A., Pye, H. O. T., Crounse, J. D., Wennberg, P. O., Flagan, R. C., and Seinfeld, J. H.: Secondary organic aerosol (SOA) formation from reaction of isoprene with nitrate radicals (NO_3), *Atmos. Chem. Phys.*, 8, 4117–4140, doi:10.5194/acp-8-4117-2008, 2008.
- 20 Odum, J. R., Hoffmann, T., Bowman, F., Collins, D., Flagan, R. C., and Seinfeld, J. H.: Gas/particle partitioning and secondary organic aerosol yields, *Environ. Sci. Technol.*, 30, 2580–2585, 1996.
- Pöschl, U., Martin, S. T., Sinha, B., Chen, Q., Gunthe, S. S., Huffman, J. A., Borrmann, S., Farmer, D. K., Garland, R. M., Helas, G., Jimenez, J. L., King, S. M., Manzi, A., Mikhailov, E., Pauliquevis, T., Petters, M. D., Prenni, A. J., Roldin, P., Rose, D., Schneider, J., Su, H., Zorn, S. R., Artaxo, P., and Andreae, M. O.: Rainforest aerosols as biogenic nuclei of clouds and precipitation in the Amazon. *Science*, 329, 1513–1516, doi:10.1126/science.1191056, 2010.
- 25 Putaud, J.-P., Raes, F., Van Dingenen, R., Brüggemann, E., Facchini, M. C., Decesari, S., Fuzzi, S., Gehrig, R., Hüglin, C., Laj, P., Lorbeer, G., Maenhaut, W., Mihalopoulos, N., Miller, K., Querol, X., Rodriguez, S., Schneider, J., Spindler, G., ten Brink, H., Trseth, K., and Wiedensohler, A.: European aerosol phenomenology: 2. Chemical characteristics of par-

Aerosol mass spectrometer constraint on the global SOA budget

D. V. Spracklen et al.

[Title Page](#)

[Abstract](#)

[Introduction](#)

[Conclusions](#)

[References](#)

[Tables](#)

[Figures](#)

◀

▶

◀

▶

[Back](#)

[Close](#)

[Full Screen / Esc](#)

[Printer-friendly Version](#)

[Interactive Discussion](#)



Aerosol mass spectrometer constraint on the global SOA budget

D. V. Spracklen et al.

[Title Page](#)[Abstract](#)[Introduction](#)[Conclusions](#)[References](#)[Tables](#)[Figures](#)[◀](#)[▶](#)[◀](#)[▶](#)[Back](#)[Close](#)[Full Screen / Esc](#)[Printer-friendly Version](#)[Interactive Discussion](#)

- ticulate matter at kerbside, urban, rural and background sites in Europe, *Atmos. Environ.*, 38(16), 2579–2595, doi:10.1016/j.atmosenv.2004.01.041, 2004.
- Pye, H. O. T. and Seinfeld, J. H.: A global perspective on aerosol from low-volatility organic compounds, *Atmos. Chem. Phys.*, 10, 4377–4401, doi:10.5194/acp-10-4377-2010, 2010.
- Rap, A., Forster, P. M., Jones, A., Boucher, O., Haywood, J. M., Bellouin, N., and De Leon, R. R.: Parameterisation of contrails in the UK Met Office Climate Model, *J. Geophys. Res.*, 115, D10205, doi:10.1029/2009JD012443, 2010.
- Robinson, A. L., Donahue, N. M., Shrivastava, M. K., Weitkamp, E. A., Sage, A. M., Grieshop, A. P., Lane, T. E., Pierce, J. R., and Pandis, S. N.: Rethinking organic aerosols: Semivolatile emissions and photochemical ageing, *Science*, 315(5816), 1259–1262, 2007.
- Robinson, N. H., Hamilton, J. F., Allan, J. D., Langford, B., Oram, D. E., Chen, Q., Docherty, K., Farmer, D. K., Jimenez, J. L., Ward, M. W., Hewitt, C. N., Barley, M. H., Jenkin, M. E., Rickard, A. R., Martin, S. T., McFiggans, G., and Coe, H.: Evidence for a significant proportion of Secondary Organic Aerosol from isoprene above a maritime tropical forest, *Atmos. Chem. Phys.*, 11, 1039–1050, doi:10.5194/acp-11-1039-2011, 2011.
- Rossow, W. B. and Schiffer, R. A.: Advances in understanding clouds from ISCCP, *B. Am. Meteorol. Soc.*, 80, 2261–2288, 1999.
- Schichtel, B. A.: Fossil and contemporary fine particulate carbon fractions at 12 rural and urban sites in the United States, *J. Geophys. Res.-Atmos.*, 113, D02311, doi:10.1029/2007JD008605, 2008.
- Slowik, J. G., Stroud, C., Bottenheim, J. W., Brickell, P. C., Chang, R. Y.-W., Liggio, J., Makar, P. A., Martin, R. V., Moran, M. D., Shantz, N. C., Sjostedt, S. J., van Donkelaar, A., Vlasenko, A., Wiebe, H. A., Xia, A. G., Zhang, J., Leaitch, W. R., and Abbatt, J. P. D.: Characterization of a large biogenic secondary organic aerosol event from eastern Canadian forests, *Atmos. Chem. Phys.*, 10, 2825–2845, doi:10.5194/acp-10-2825-2010, 2010.
- Spracklen, D. V., Pringle, K. J., Carslaw, K. S., Chipperfield, M. P., and Mann, G. W.: A global off-line model of size-resolved aerosol microphysics: I. Model development and prediction of aerosol properties, *Atmos. Chem. Phys.*, 5, 2227–2252, doi:10.5194/acp-5-2227-2005, 2005a.
- Spracklen, D. V., Pringle, K. J., Carslaw, K. S., Chipperfield, M. P., and Mann, G. W.: A global off-line model of size-resolved aerosol microphysics: II. Identification of key uncertainties, *Atmos. Chem. Phys.*, 5, 3233–3250, doi:10.5194/acp-5-3233-2005, 2005b.
- Spracklen, D. V., Carslaw, K. S., Kulmala, M., Kerminen, V.-M., Mann, G. W., and Sihto, S.-

Aerosol mass spectrometer constraint on the global SOA budget

D. V. Spracklen et al.

[Title Page](#)

[Abstract](#)

[Introduction](#)

[Conclusions](#)

[References](#)

[Tables](#)

[Figures](#)



[◀](#)

[▶](#)

[Back](#)

[Close](#)

[Full Screen / Esc](#)

[Printer-friendly Version](#)

[Interactive Discussion](#)



Aerosol mass spectrometer constraint on the global SOA budget

D. V. Spracklen et al.

[Title Page](#)[Abstract](#)[Introduction](#)[Conclusions](#)[References](#)[Tables](#)[Figures](#)[◀](#)
[Back](#)[▶](#)
[Close](#)[Full Screen / Esc](#)[Printer-friendly Version](#)[Interactive Discussion](#)

Tsigaridis, K., Krol, M., Dentener, F. J., Balkanski, Y., Lathière, J., Metzger, S., Hauglustaine, D. A., and Kanakidou, M.: Change in global aerosol composition since preindustrial times, *Atmos. Chem. Phys.*, 6, 5143–5162, doi:10.5194/acp-6-5143-2006, 2006.

Tsigaridis, K. and Kanakidou, M.: Secondary organic aerosol importance in the future atmosphere, *Atmos. Environ.*, 41, 4682–4692, 2007.

Tsimpidi, A. P., Karydis, V. A., Zavala, M., Lei, W., Molina, L., Ulbrich, I. M., Jimenez, J. L., and Pandis, S. N.: Evaluation of the volatility basis-set approach for the simulation of organic aerosol formation in the Mexico City metropolitan area, *Atmos. Chem. Phys.*, 10, 525–546, doi:10.5194/acp-10-525-2010, 2010.

10 Tunved, P., Hansson, H.-C., Kerminen, V.-M., Ström, J., Dal Maso, M., Lihavainen, H., Viisanen, Y., Aalto, P. P., Komppula, M., and Kulmala, M.: High natural aerosol loading over boreal forests, *Science*, 312, 261–263, doi:10.1126/science.1123052, 2006.

Turpin, B. J. and Lim, H. J.: Species contributions to PM_{2.5} mass concentrations: Revisiting common assumptions for estimating organic mass, *Aerosol Sci. Technol.*, 35(1), 602–610, 2001.

15 Ulbrich, I. M., Canagaratna, M. R., Zhang, Q., Worsnop, D. R., and Jimenez, J. L.: Interpretation of organic components from Positive Matrix Factorization of aerosol mass spectrometric data, *Atmos. Chem. Phys.*, 9, 2891–2918, doi:10.5194/acp-9-2891-2009, 2009.

Weber, R. J., Sullivan, A. P., Peltier, R. E., Russell, A., Yan, B., Zheng, M., de Gouw, J., Warneke, C., Brock, C., Holloway, J. S., Atlas, E. L., and Edgerton, E.: A study of secondary organic aerosol formation in the anthropogenic-influenced southeastern United States, *J. Geophys. Res.*, 112, D13302, doi:10.1029/2007JD008408, 2007.

Virtanen, A., Joutsensaari, J., Koop, T., Kannisto, J., Yli-Pirilä, P., Leskinen, J., Mäkelä, J. M., Holopainen, J. K., Pöschl, U., Kulmala, M., Worsnop, D. R., and Laaksonen, A.: An amorphous solid state of biogenic secondary organic aerosol particles, *Nature*, 467, 824–827, doi:10.1038/nature09455, 2010.

20 Volkamer, R., Jimenez, J. L., San Martini, F., Dzepina, K., Zhang, Q., Salcedo, D., Molina, L. T., Worsnop, D. R., and Molina, M. J.: Secondary organic aerosol formation from anthropogenic air pollution: Rapid and higher than expected, *Geophys. Res. Lett.*, 33, L17811, doi:10.1029/2006GL026899, 2006.

Yassaa, N., Peeken, I., Zollner, E., Bluhm, K., Arnold, S., Spracklen, D. and Williams, J.: Evidence for marine production of monoterpenes, *Environ. Chem.*, 5(6), 391–401, 2008.

30 Yokelson, R. J., Crounse, J. D., DeCarlo, P. F., Karl, T., Urbanski, S., Atlas, E., Campos, T.,

Shinozuka, Y., Kapustin, V., Clarke, A. D., Weinheimer, A., Knapp, D. J., Montzka, D. D., Holloway, J., Weibring, P., Flocke, F., Zheng, W., Toohey, D., Wennberg, P. O., Wiedinmyer, C., Mauldin, L., Fried, A., Richter, D., Walega, J., Jimenez, J. L., Adachi, K., Buseck, P. R., Hall, S. R., and Shetter, R.: Emissions from biomass burning in the Yucatan, *Atmos. Chem. Phys.*, 9, 5785–5812, doi:10.5194/acp-9-5785-2009, 2009.

Zhang, Q., Worsnop, D. R., Canagaratna, M. R., and Jimenez, J. L.: Hydrocarbon-like and oxygenated organic aerosols in Pittsburgh: insights into sources and processes of organic aerosols, *Atmos. Chem. Phys.*, 5, 3289–3311, doi:10.5194/acp-5-3289-2005, 2005.

Zhang, Q., Jimenez, J. L., Canagaratna, M. R., Allan, J. D., Coe, H., Ulbrich, I., Alfarra, M. R., Takami, A., Middlebrook, A. M., Sun, Y. L., Dzepina, K., Dunlea, E., Docherty, K., DeCarlo, P. F., Salcedo, D., Onasch, T., Jayne, J. T., Miyoshi, T., Shimono, A., Hatakeyama, S., Takegawa, N., Kondo, Y., Schneider, J., Drewnick, F., Borrmann, S., Weimer, S., Demerjian, K., Williams, P., Bower, K., Bahreini, R., Cottrell, L., Griffin, R. J., Rautiainen, J., Sun, J. Y., Zhang, Y. M., and Worsnop, D. R.: Ubiquity and dominance of oxygenated species in organic aerosols in anthropogenically-influenced Northern Hemisphere midlatitudes, *Geophys. Res. Lett.*, 34, L13801, doi:10.1029/2007GL029979, 2007.

Aerosol mass spectrometer constraint on the global SOA budget

D. V. Spracklen et al.

[Title Page](#)

[Abstract](#)

[Introduction](#)

[Conclusions](#)

[References](#)

[Tables](#)

[Figures](#)

◀

▶

[Back](#)

[Close](#)

[Full Screen / Esc](#)

[Printer-friendly Version](#)

[Interactive Discussion](#)



Aerosol mass spectrometer constraint on the global SOA budget

D. V. Spracklen et al.

Table 1. Reactions of VOCs: anthropogenic (VOC_A), biomass burning (VOC_{BB}) and biogenic (isoprene and α -pinene; VOC_B) to produce an assumed condensable product (SOA_g) with molar yield (y1 to y10). The reaction rate of Reactions (7–10) were scaled by a linear factor (r7 through r10).

	Reaction	Rate constant
1	α -pinene + OH \rightarrow y1. SOAg	$1.2 \times 10^{-11} \exp(444/T)$
2	α -pinene + O ₃ \rightarrow y2. SOAg	$1.01 \times 10^{-15} \exp(-732/T)$
3	α -pinene + NO ₃ \rightarrow y3. SOAg	$1.19 \times 10^{-12} \exp(490/T)$
4	isoprene + OH \rightarrow y4. SOAg	$2.7 \times 10^{-11} \exp(390/T)$
5	isoprene + O ₃ \rightarrow y5. SOAg	$1 \times 10^{-14} \exp(-1995/T)$
6	isoprene + NO ₃ \rightarrow y6. SOAg	$3.15 \times 10^{-12} \exp(-450/T)$
7	VOC _A + OH \rightarrow y7. SOAg	$5 \times 10^{-12} \times r7$ (*)
8	VOC _{BB} + OH \rightarrow y8. SOAg	$5 \times 10^{-12} \times r8$
9	VOC _B + VOC _A \rightarrow y9. SOAg + VOC _A	$5 \times 10^{-16} \times r9$
10	VOC _B + SO ₂ \rightarrow y10. SOAg + SO ₂	$1 \times 10^{-14} \times r10$

(*): this estimated rate is based on the summaries of field observations by de Gouw et al. (2008) and DeCarlo et al. (2010).

[Title Page](#)

[Abstract](#)

[Introduction](#)

[Conclusions](#)

[References](#)

[Tables](#)

[Figures](#)

◀

▶

◀

▶

[Back](#)

[Close](#)

[Full Screen / Esc](#)

[Printer-friendly Version](#)

[Interactive Discussion](#)



Aerosol mass spectrometer constraint on the global SOA budget

D. V. Spracklen et al.

[Title Page](#)

[Abstract](#)

[Introduction](#)

[Conclusions](#)

[References](#)

[Tables](#)

[Figures](#)

[◀](#)

[▶](#)

[◀](#)

[▶](#)

[Back](#)

[Close](#)

[Full Screen / Esc](#)

[Printer-friendly Version](#)

[Interactive Discussion](#)

Table 2. Summary statistics for the evaluation of simulated sulfate, OA, HOA and OOA against AMS observations with comparison at sites classified as remote in parenthesis. The SOA source from monoterpenes (S_M), isoprene (S_I), anthropogenic VOC (S_A), biomass burning VOC (S_{BB}) and from oxidation of POA to SOA (S_P), are detailed for each simulation.

#	SOA yield (y), reaction rate (r), and POA half-life (τ_p) ^a	Global SOA source ^b / Tg (SOA) a ⁻¹					Summary statistics ^c		
		S_M	S_I	S_A	S_{BB}	S_P	NMB/%	NME/%	R^2
Comparison against observed sulfate									
1		N/A	N/A	N/A	N/A	N/A	18 (10)	66 (65)	0.36 (0.26)
Comparison against observed OA									
1	y1-3=26%	32.3	0.	0.	0.	0.	-68 (-51)	74 (67)	0.27 (0.12)
33	Optimised yields	6.5	6.5	100	3	23.	-12 (28)	59 (53)	0.31 (0.43)
Comparison against observed OOA									
1	y1-3=26%	32.3	0.	0.	0.	0.	-85 (-80)	87 (87)	0.00 (0.02)
2	y1-3=130%	161.5	0.	0.	0.	0.	-24 (-3)	94 (125)	0.00 (0.02)
3	y1-3=198%	246.0	0.	0.	0.	0.	16 (48)	118 (160)	0.00 (0.02)
4	y1-3=26%, y4-6=6%	32.3	26.2	0.	0.	0.	-77 (-70)	85 (91)	0.00 (0.02)
5	y1-3=26%, y4-6=12%	32.3	52.4	0.	0.	0.	-68 (-59)	85 (96)	0.00 (0.02)
6	y1-3=26%, y4-6=6%, y8=90%	32.3	26.2	0.0	42.3	0.	-71 (-61)	81 (85)	0.03 (0.00)
7	y1-3=26%, y4-6=6%, y8=180%	32.3	26.2	0.0	84.6	0.	-65 (-51)	82 (88)	0.03 (0.00)

Aerosol mass spectrometer constraint on the global SOA budget

D. V. Spracklen et al.

[Title Page](#)

[Abstract](#)

[Introduction](#)

[Conclusions](#)

[References](#)

[Tables](#)

[Figures](#)

[◀](#)

[▶](#)

[◀](#)

[▶](#)

[Back](#)

[Close](#)

[Full Screen / Esc](#)

[Printer-friendly Version](#)

[Interactive Discussion](#)

Table 2. Continued.

#	SOA yield (y), reaction rate (r), and POA half-life (τ_p) ^a	Global SOA source ^b / Tg (SOA) a ⁻¹					Summary statistics ^c		
		S_M	S_I	S_A	S_{BB}	S_P	NMB/%	NME/%	R^2
8	y1-3=26%, y4-6=6%, τ_p = 1 day	32.3	26.2	0.	0.	79.	-64 (-52)	75 (80)	0.10 (0.00)
9	y1-3=16%, y4-6=6%, τ_p = 2.7 days	32.3	26.2	0.	0.	65.	-68 (-57)	78 (83)	0.06 (0.00)
10	y1-3=26%, y4-5=6%, τ_p = 8 days	32.3	26.2	0.	0.	39.5	-72 (-63)	81 (86)	0.02 (0.00)
11	y1-3=26%, y4-6=6%, y7=30%	32.3	26.2	38.	0.	0.	-51 (-40)	67 (77)	0.08 (0.03)
12	y1-3=26%, y4-6=6%, y7=60%	32.3	26.2	76.	0.	0.	-25 (-10)	59 (63)	0.13 (0.13)
13	y1-3=26%, y7=30%	32.3	0.	38.	0.	0.	-59 (-50)	68 (72)	0.10 (0.09)
14	y1-3=26%, y7=60%	32.3	0.	76.	0.	0.	-33 (-20)	55 (58)	0.16 (0.21)
15	y1-3=26%, y7=90%	32.3	0.	114.	0.	0.	-8 (9)	57 (52)	0.19 (0.29)
16	y7=90%	0.0	0.	114.	0.	0.	-23 (-10)	50 (41)	0.25 (0.51)
17	y1-3=26%, y4-5=6%, y7=30%, y8=90%	32.3	26.2	38.	42.3	0.	-45 (-30)	64 (73)	0.11 (0.04)
18	y1-3=26%, y7=30%, r7=10	32.3	0.	38.8	0.	0.	-50 (-44)	60 (70)	0.10 (0.10)

Aerosol mass spectrometer constraint on the global SOA budget

D. V. Spracklen et al.

[Title Page](#)

[Abstract](#)

[Introduction](#)

[Conclusions](#)

[References](#)

[Tables](#)

[Figures](#)

◀

▶

◀

▶

[Back](#)

[Close](#)

[Full Screen / Esc](#)

[Printer-friendly Version](#)

[Interactive Discussion](#)

Table 2. Continued.

#	SOA yield (y), reaction rate (r), and POA half-life (τ_p) ^a	Global SOA source ^b / Tg(SOA) a ⁻¹					Summary statistics ^c		
		S _M	S _I	S _A	S _{BB}	S _P	NMB/%	NME/%	R ²
19	y1-3=26%, y7=60%, r7=10	32.3	0.	77.6	0.	0.	-15 (-8)	60 (60)	0.14 (0.20)
20	y1-3=26%, y7=90%, r7=10	32.3	0.	116.	0.	0.	20 (27)	75 (64)	0.16 (0.25)
21	y1-3=26%, y7=30%, r7=100	32.3	0.	39.	0.	0.	-42 (-40)	61 (69)	0.09 (0.09)
22	y1-3=26%, y7=60%, r7=100	32.3	0.	78.	0.	0.	1 (1)	71 (64)	0.12 (0.17)
23	y1-3=26%, y7=90%, r7=100	32.3	0.	117.	0.	0.	44 (42)	93 (78)	0.12 (0.21)
24	y1-2=26%, y3=130%	104.8	0.0	0.	0.	0.	-50 (-36)	85 (105)	0.00 (0.02)
25	y1,3=26%, y2=130%	44.9	0.0	0.	0.	0.	-78 (-71)	85 (89)	0.00 (0.01)
26	y1=130%, y2-3=36%	53.4	0.0	0.	0.	0.	-65 (-55)	83 (96)	0.00 (0.02)
27	y1-y3=26%, y10=130%, r10=1	39.6	0.0	0.	0.	0.	-73 (-70)	81 (88)	0.01 (0.00)
28	y1-y3=26%, y10=130%, r10=10	63.4	0.0	0.	0.	0.	-50 (-44)	80 (97)	0.00 (0.00)
29	y1-3=26%, y4-6=6%, r9=1, y9=100%	63	0.	0.	0.	0.	-71 (-65)	82 (92)	0.00 (0.02)

Aerosol mass spectrometer constraint on the global SOA budget

D. V. Spracklen et al.

[Title Page](#)

[Abstract](#)

[Introduction](#)

[Conclusions](#)

[References](#)

[Tables](#)

[Figures](#)

[◀](#)

[▶](#)

[◀](#)

[▶](#)

[Back](#)

[Close](#)

[Full Screen / Esc](#)

[Printer-friendly Version](#)

[Interactive Discussion](#)



Table 2. Continued.

#	SOA yield (y), reaction rate (r), and POA half-life (τ_p) ^a	Global SOA source ^b / Tg (SOA) a ⁻¹				Summary statistics ^c			
		S_M	S_I	S_A	S_{BB}	S_P	NMB/%	NME/%	R^2
30	y1-3=26%, y4-6=6%, r9=10, y9=100%	99.	0.	0.	0.	0.	-32 (-25)	87 (105)	0.02 (0.00)
31	y1-3=26%, y4-6=6%, r9=10, y9=50%	78.3	0.	0.	0.	0.	-54 (-48)	80 (96)	0.01 (0.00)
32	y1-3=26%, y4-6=6%, r9=10; y9=20%	65.8	0.	0.	0.	0.	-68 (-62)	81 (93)	0.00 (0.01)
33	Optimised yields	6.5	6.5	100.	23.	3.	-11 (5)	53 (46)	0.23 (0.37)
Comparison against observed HOA									
1	N/A	N/A	N/A	N/A	N/A	N/A	-16 (274)	85 (274)	0.27 (0.65)
16	τ_p = 1 day	N/A	N/A	N/A	N/A	79	-60 (45)	73 (73)	0.41 (0.71)
17	τ_p = 2.7 days	N/A	N/A	N/A	N/A	65	-46 (114)	74 (122)	0.37 (0.70)
18	τ_p = 8 days	N/A	N/A	N/A	N/A	35	31 (190)	78 (194)	0.31 (0.67)

^a Reactions specified in Table 1. SOA yields (y1–y10) are defined as the SOA mass as a fraction of the VOC mass expressed as a percentage. They are specified when they are non-zero. In simulations 16–18 POA is aged to SOA assuming a first order rate constant. We specify the half life (τ_p) of POA with respect to ageing to SOA. ^b Conversion factor of 2 Tg (SOA): 1 Tg (C). ^c Normalised mean bias (NMB) = $100\% \times \sum (M_i - O_i)/\sum O_i$; normalised mean error (NME) = $100\% \times \sum |M_i - O_i|/\sum O_i$ and correlation coefficient (R^2) between model (M_i) and observations (O_i) where i represents a given study in the AMS dataset.

Table 3. Summary of the location, time and duration of the AMS studies, additional to those described in Zhang et al. (2007), that were used in our analysis. All additional sites were classified as remote.

Dataset name	Location	Lon.	Lat.	Elevation (m)	Time Period	Season	Previous publications/ Acknowledgments
OP3	Bukit Atur, Sabah, Malaysia	117.8	5.0	426	06/21/2008–07/24/2008	Wet	Hewitt et al. (2010); Robinson et al. (2011)
AMAZE	Near Manaus, Amazon	-60.2	-2.6	100	02/07/2008–03/13/2008	Wet	Chen et al. (2009); Pöschl et al. (2010)
Whistler Trinidad Head Thompson Farm Whiteface Mtn.	Whistler Peak, BC, Canada Trinidad Head, CA, USA Thompson Farm, NH, USA Whiteface Mountains, NY, USA	-122.9 -124.1 -70.9 -73.8	50.0 41.1 43.1 44.4	2181 107 24 600	04/20/2006–05/17/2006 04/20/2002–05/20/2002 07/09/2005–08/15/2005 07/09/2002–08/07/2002	Summer Summer Summer Summer	Sun et al. (2009) Allan et al. (2004) Cottrell et al. (2008) F. Drewnick & K. Demerjian ASRC, UAlbany Yin-Nan Lee & L. Kleinman, Brookhaven National Laboratory
VOCALS	Southeast Pacific	-72.5	-18.9	413	10/14/2008–11/13/2008		Capes et al. (2009)
AMMA DABEX DABEX	West Africa West Africa West Africa	2.2 4.0 -17.0	13.5 13.0 12.0	<2000 <2000 <2000	07/17/2008–08/18/2008 01/13/2006–02/03/2006 01/13/2006–02/03/2006		Capes et al. (2008) Capes et al. (2008) Capes et al. (2008)

[Title Page](#)[Abstract](#)[Introduction](#)[Conclusions](#)[References](#)[Tables](#)[Figures](#)[◀](#)[▶](#)[◀](#)[▶](#)[Back](#)[Close](#)[Full Screen / Esc](#)[Printer-friendly Version](#)[Interactive Discussion](#)

Aerosol mass spectrometer constraint on the global SOA budget

D. V. Spracklen et al.

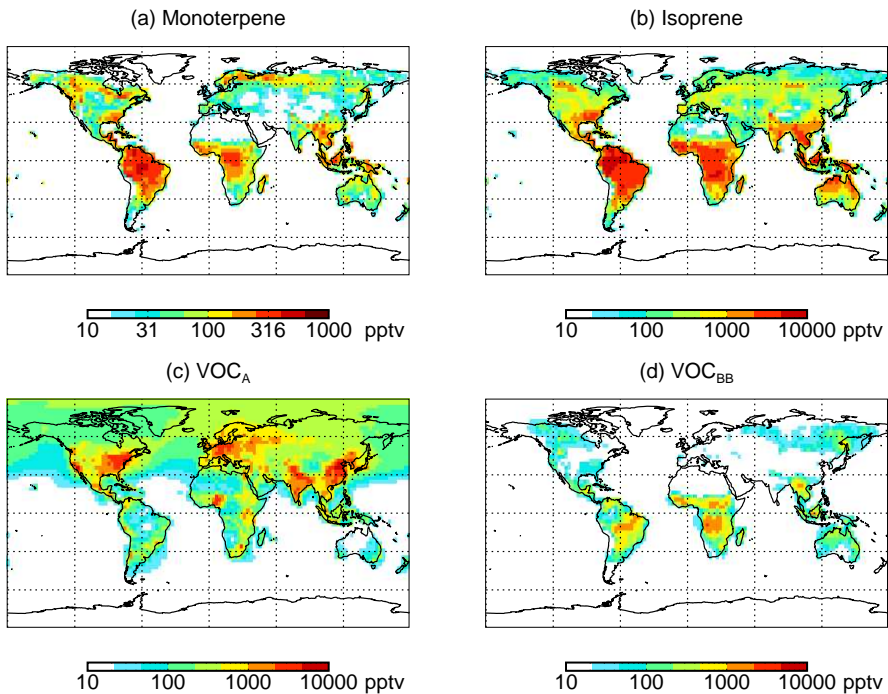


Fig. 1. Simulated annual mean surface concentrations of (a) monoterpene, (b) isoprene, (c) anthropogenic VOC (VOC_A), (d) biomass burning VOC (VOC_{BB}).

[Title Page](#)[Abstract](#)[Introduction](#)[Conclusions](#)[References](#)[Tables](#)[Figures](#)[Back](#)[Close](#)[Full Screen / Esc](#)[Printer-friendly Version](#)[Interactive Discussion](#)

Aerosol mass spectrometer constraint on the global SOA budget

D. V. Spracklen et al.

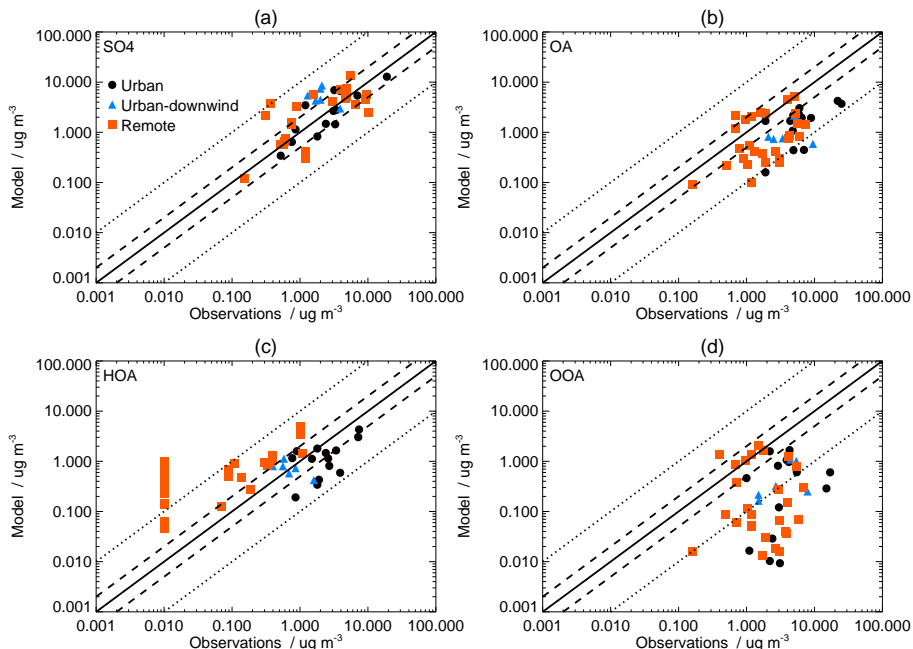


Fig. 2. Scatterplot of simulated (GLOMAP, simulation 1) versus observed (AMS) (a) sulfate, (b) OA, (c) HOA and (d) OOA. Model includes SOA from monoterpene (26% SOA yield, $32.3 \text{ Tg (SOA) a}^{-1}$). Observation locations are classified as urban, urban-downwind and rural/remote as in Zhang et al. (2007). The 1:1 line (solid), 2:1 lines (dashed) and 10:1 lines (dotted) are indicated. Model-observation statistics are shown in Table 2. Observational constraints limit identification of HOA at very low concentrations. We assume a lower limit for HOA of $0.01 \mu\text{g m}^{-3}$.

- [Title Page](#)
- [Abstract](#) [Introduction](#)
- [Conclusions](#) [References](#)
- [Tables](#) [Figures](#)
- [◀](#) [▶](#)
- [◀](#) [▶](#)
- [Back](#) [Close](#)
- [Full Screen / Esc](#)
- [Printer-friendly Version](#)
- [Interactive Discussion](#)

Aerosol mass spectrometer constraint on the global SOA budget

D. V. Spracklen et al.

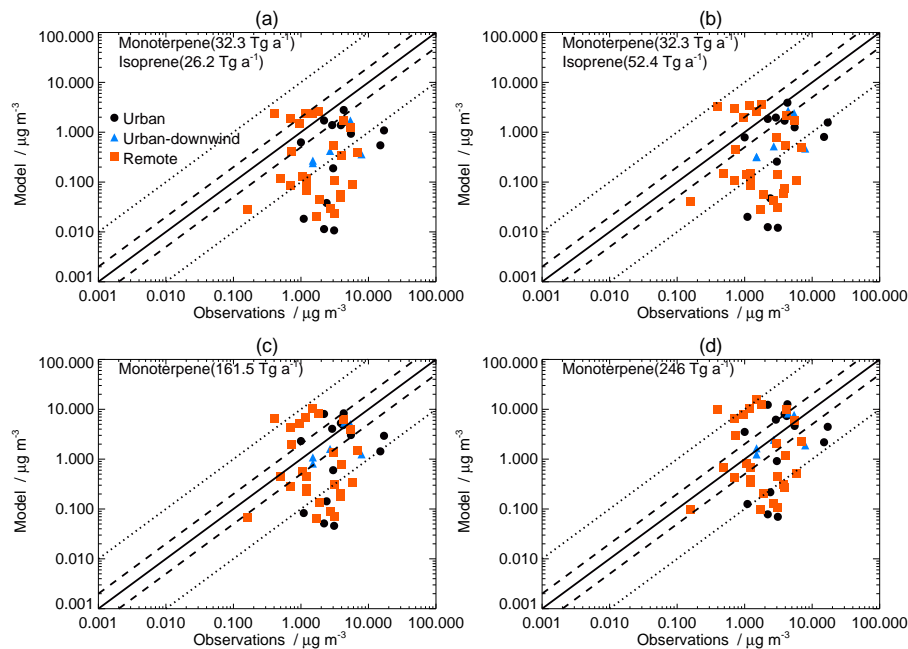


Fig. 3. As for Fig. 2 but for simulated versus observed OOA for **(a)** simulation 4: monoterpene (32.3 Tg (SOA) a^{-1}), isoprene (26.2 Tg (SOA) a^{-1}); **(b)** simulation 5: monoterpene (32.3 Tg (SOA) a^{-1}), isoprene (52.4 Tg (SOA) a^{-1}); **(c)** simulation 2: monoterpene (161.5 Tg (SOA) a^{-1}); **(d)** simulation 3: monoterpene (246. Tg (SOA) a^{-1}).

Aerosol mass spectrometer constraint on the global SOA budget

D. V. Spracklen et al.

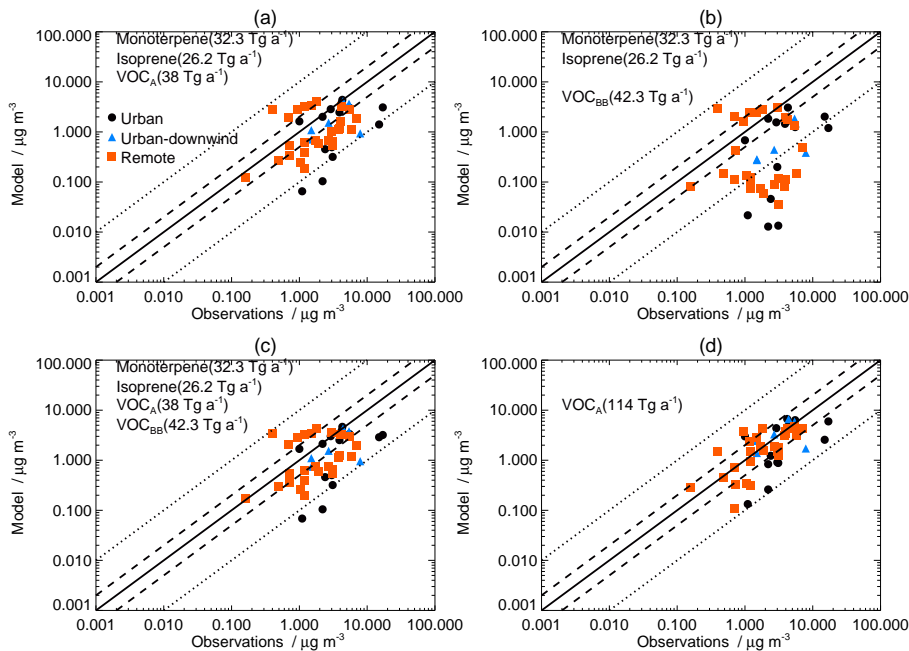


Fig. 4. As for Fig. 3, but for (a) simulation 11: monoterpene ($32.3 \text{ Tg (SOA) } \text{a}^{-1}$), isoprene ($26.2 \text{ Tg (SOA) } \text{a}^{-1}$), anthropogenic VOC ($38. \text{ Tg (SOA) } \text{a}^{-1}$); (b) simulation 6: monoterpene ($32.3 \text{ Tg (SOA) } \text{a}^{-1}$), isoprene ($26.2 \text{ Tg (SOA) } \text{a}^{-1}$), biomass burning VOC ($42.3 \text{ Tg (SOA) } \text{a}^{-1}$); (c) simulation 17: monoterpene ($32.3 \text{ Tg (SOA) } \text{a}^{-1}$), isoprene ($26.2 \text{ Tg (SOA) } \text{a}^{-1}$), anthropogenic VOC ($38. \text{ Tg (SOA) } \text{a}^{-1}$), biomass burning VOC ($42.3 \text{ Tg (SOA) } \text{a}^{-1}$); (d) simulation 15: anthropogenic VOC ($114. \text{ Tg (SOA) } \text{a}^{-1}$).

Aerosol mass spectrometer constraint on the global SOA budget

D. V. Spracklen et al.

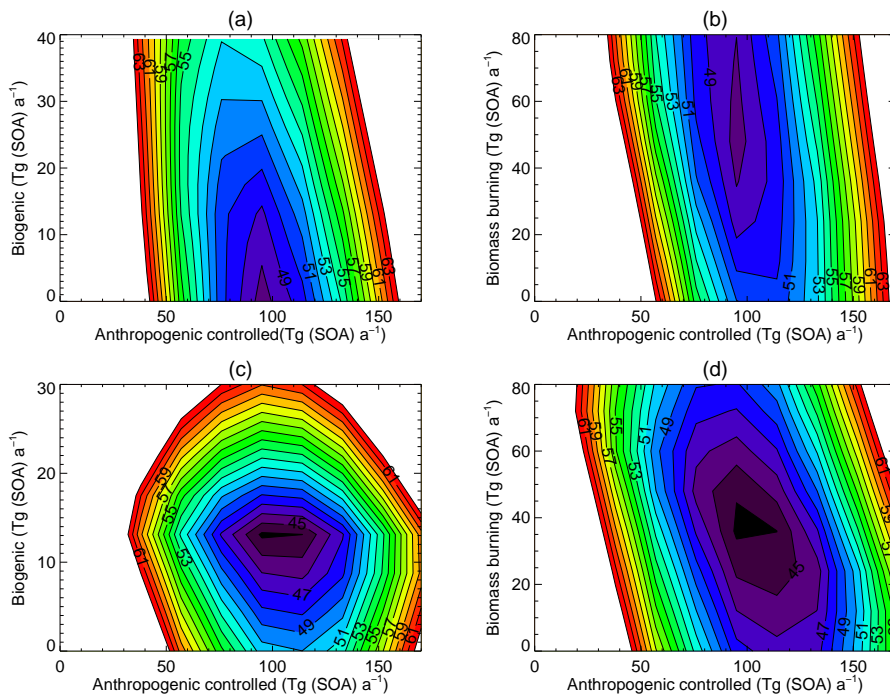


Fig. 5. Normalised mean error (NME, %) between SOA simulated by a linear version of the global model and OOA observed by the AMS as a function of (**a**) and (**c**) biogenic (isoprene and monoterpene) and anthropogenically controlled SOA (biomass burning SOA fixed at 36 Tg (SOA) a⁻¹); (**b**) and (**d**) biomass burning and anthropogenic controlled SOA (biogenic SOA fixed at 13 Tg (SOA) a⁻¹). In panels (**c**) and (**d**) AMS observations have been weighted to remove bias in the observational dataset as described in Sect. 3.2.

Aerosol mass spectrometer constraint on the global SOA budget

D. V. Spracklen et al.

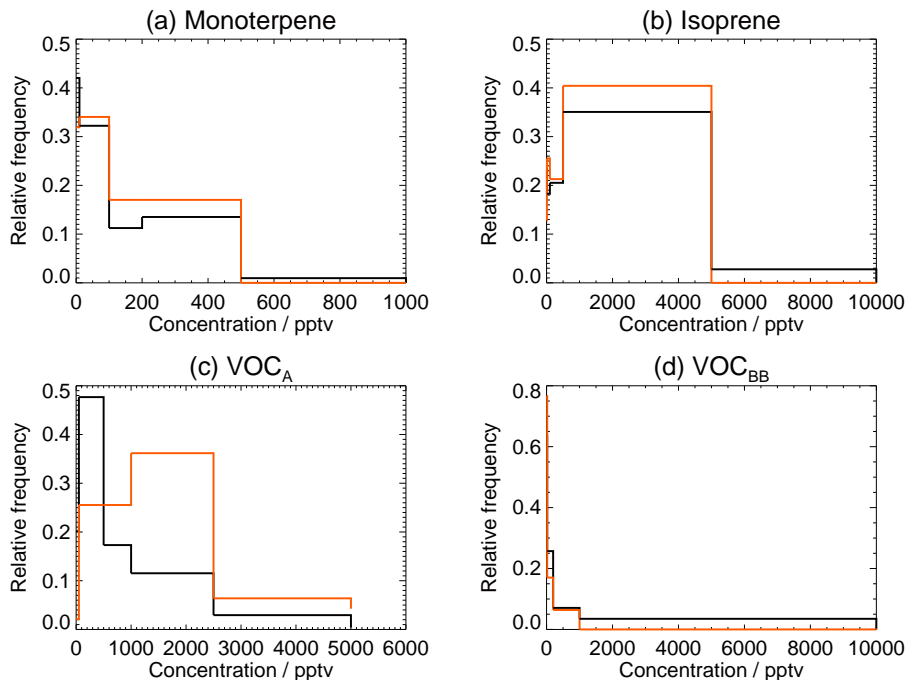


Fig. 6. Probability distribution of (a) monoterpenes, (b) isoprene, (c) anthropogenic VOC (VOC_A) and (d) biomass burning VOC (VOC_{BB}) as a function of concentration. The black line shows simulated probability distribution for all global land surface (excluding Antarctica). The orange line shows simulated distribution at the locations and times of the AMS observations.

- [Title Page](#)
- [Abstract](#) [Introduction](#)
- [Conclusions](#) [References](#)
- [Tables](#) [Figures](#)
- [◀](#) [▶](#)
- [◀](#) [▶](#)
- [Back](#) [Close](#)
- [Full Screen / Esc](#)
- [Printer-friendly Version](#)
- [Interactive Discussion](#)

Aerosol mass spectrometer constraint on the global SOA budget

D. V. Spracklen et al.

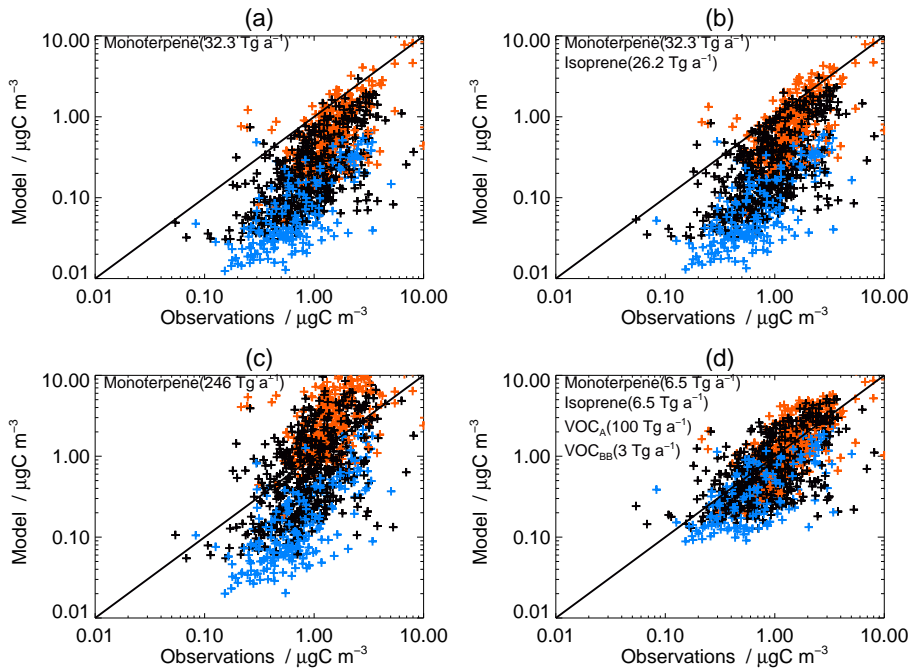


Fig. 7. Comparison between monthly mean organic carbon aerosol observed by IMPROVE and simulated by GLOMAP in the year 2000 for **(a)** Simulation 1: monoterpene ($32.3 \text{ Tg (SOA) } a^{-1}$); **(b)** Simulation 4: monoterpene ($32.3 \text{ Tg (SOA) } a^{-1}$), isoprene ($26.2 \text{ Tg (SOA) } a^{-1}$); **(c)** Simulation 3: monoterpene ($246.0 \text{ Tg (SOA) } a^{-1}$); **(d)** Simulation 34: optimised SOA sources. Winter (DJF) shown in blue, Summer (JJA) shown in red.

Aerosol mass spectrometer constraint on the global SOA budget

D. V. Spracklen et al.

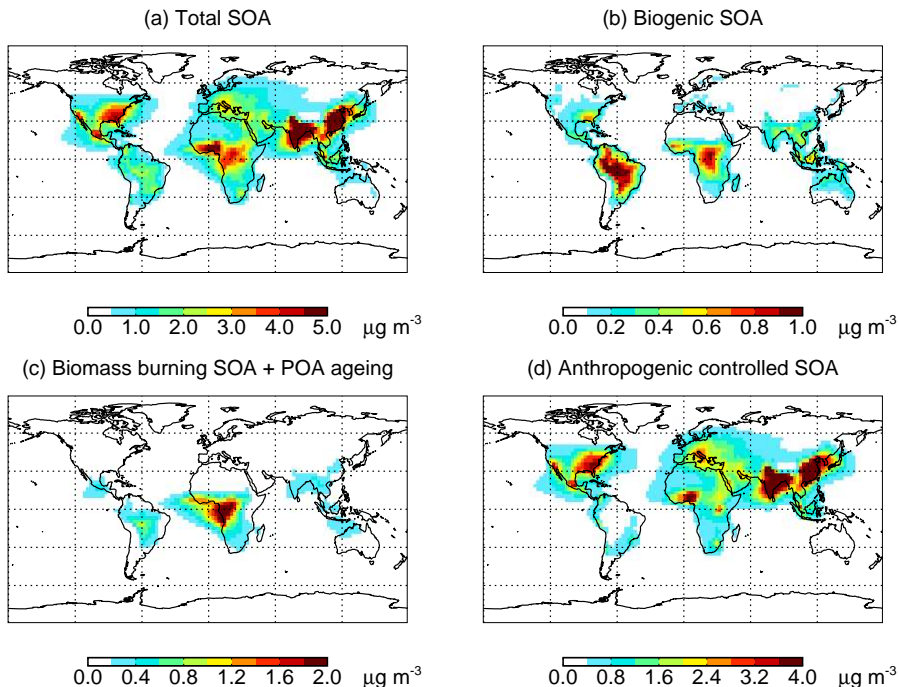


Fig. 8. Surface annual mean concentrations of SOA simulated using the optimised SOA sources: **(a)** biogenic, biomass burning, POA ageing and anthropogenic pollution controlled SOA, **(b)** biogenic SOA only, **(c)** biomass SOA and POA ageing, **(d)** anthropogenic pollution controlled SOA only. Colour scale saturates.

- [Title Page](#)
- [Abstract](#) [Introduction](#)
- [Conclusions](#) [References](#)
- [Tables](#) [Figures](#)
- [◀](#) [▶](#)
- [◀](#) [▶](#)
- [Back](#) [Close](#)
- [Full Screen / Esc](#)
- [Printer-friendly Version](#)
- [Interactive Discussion](#)

Aerosol mass spectrometer constraint on the global SOA budget

D. V. Spracklen et al.

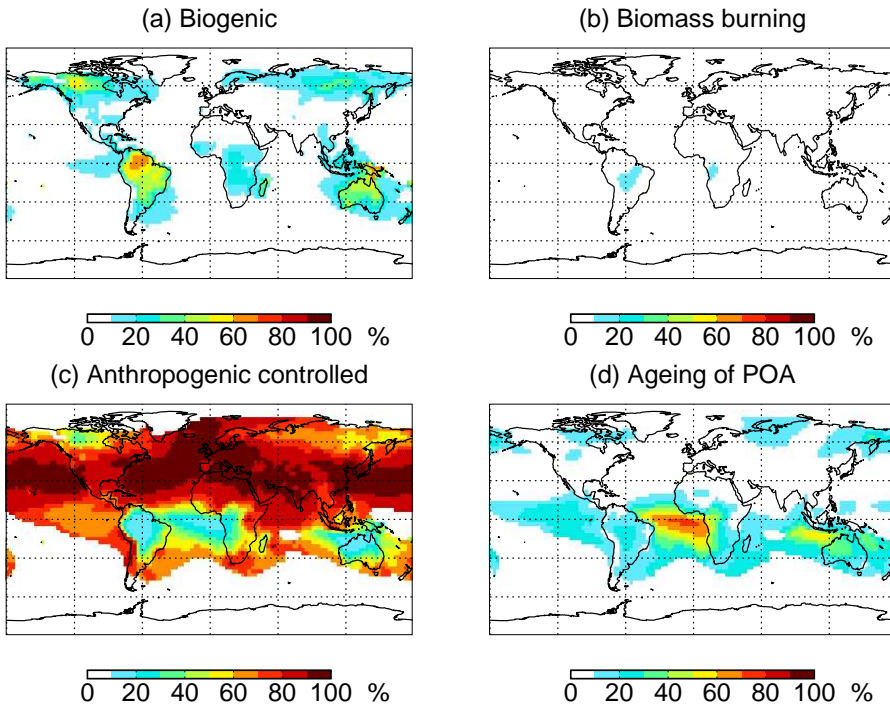


Fig. 9. Simulated fraction of simulated surface SOA concentration that is **(a)** biogenic, **(b)** biomass burning, **(c)** controlled by anthropogenic pollution, **(d)** POA to SOA ageing. Fractions are plotted where total simulated SOA is greater than $0.05 \mu\text{g m}^{-3}$.

- [Title Page](#)
- [Abstract](#) [Introduction](#)
- [Conclusions](#) [References](#)
- [Tables](#) [Figures](#)
- [◀](#) [▶](#)
- [◀](#) [▶](#)
- [Back](#) [Close](#)
- [Full Screen / Esc](#)
- [Printer-friendly Version](#)
- [Interactive Discussion](#)

Aerosol mass spectrometer constraint on the global SOA budget

D. V. Spracklen et al.

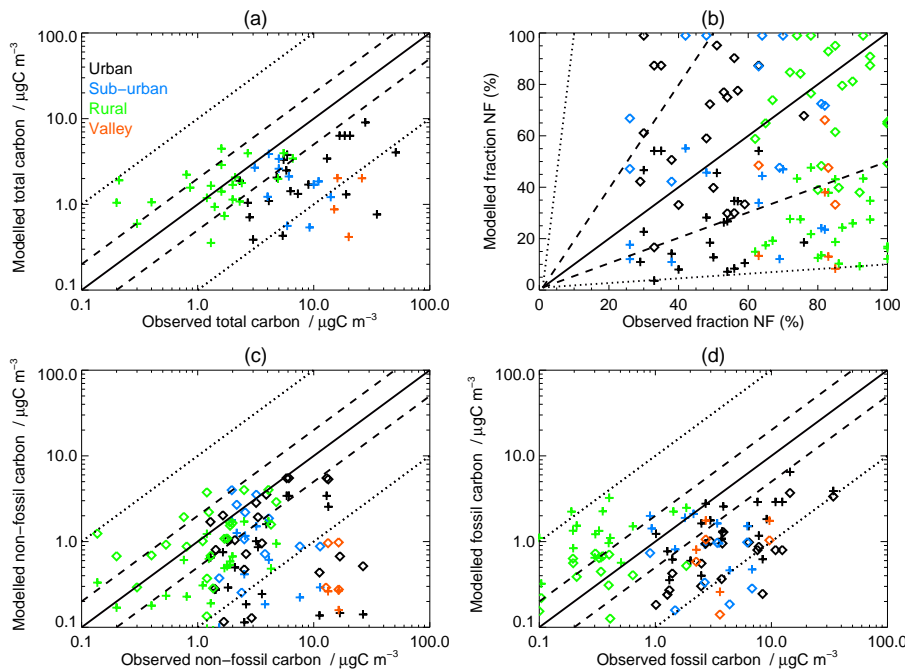


Fig. 10. Comparison of modelled and observed **(a)** total carbon aerosol, **(b)** fraction of total carbon aerosol that is non-fossil (NF), **(c)** non-fossil carbon and **(d)** fossil carbon. In panels **(b-d)** we assume that 20% (crosses) and 92% (open squares) of anthropogenically controlled SOA is non-fossil.

- [Title Page](#)
- [Abstract](#) [Introduction](#)
- [Conclusions](#) [References](#)
- [Tables](#) [Figures](#)
- [◀](#) [▶](#)
- [◀](#) [▶](#)
- [Back](#) [Close](#)
- [Full Screen / Esc](#)
- [Printer-friendly Version](#)
- [Interactive Discussion](#)

Aerosol mass spectrometer constraint on the global SOA budget

D. V. Spracklen et al.

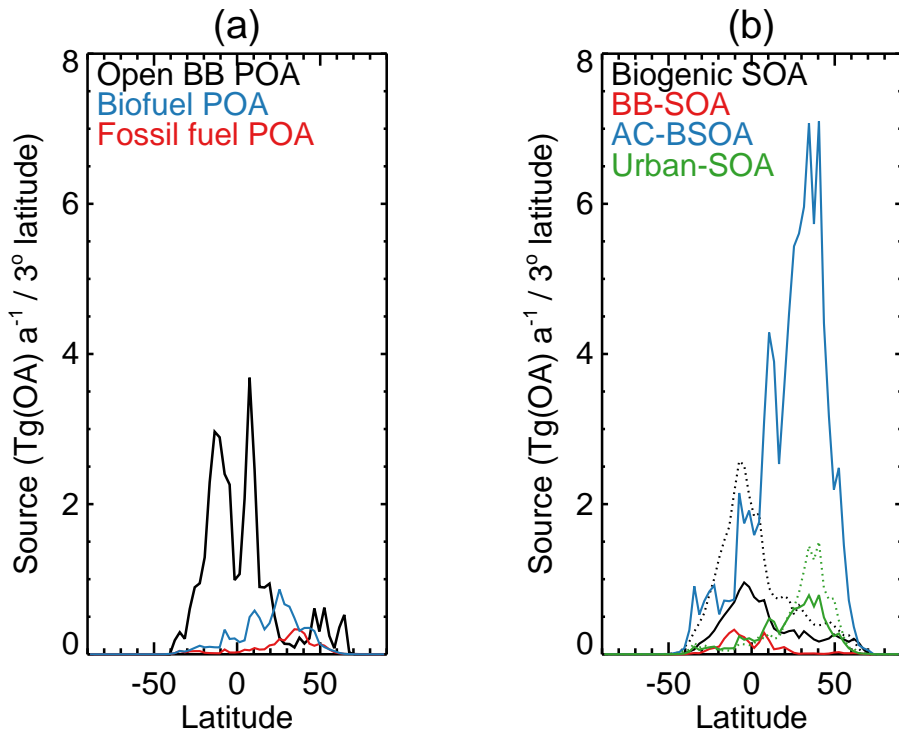


Fig. 11. Estimated zonal mean distribution of (a) POA and (b) SOA sources: biomass burning (BB-SOA); anthropogenically controlled biogenic SOA (AC-BSOA). Sources of SOA estimated in this work (solid lines) are plotted for comparison against sources estimated by de Gouw and Jimenez (2009) (dotted lines). POA emissions in the two studies are identical.

Aerosol mass spectrometer constraint on the global SOA budget

D. V. Spracklen et al.

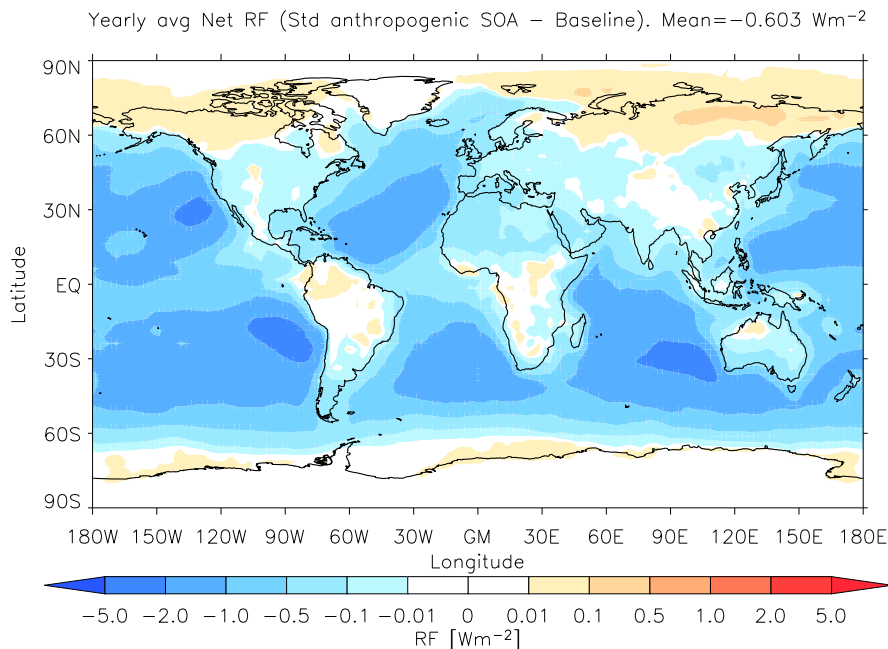


Fig. 12. Annual mean net (long wave and short wave) top of atmosphere cloud albedo radiative forcing (RF) due to anthropogenic pollution controlled SOA for a cloud updraft velocity of 0.4 m s^{-1} .

- [Title Page](#)
- [Abstract](#) [Introduction](#)
- [Conclusions](#) [References](#)
- [Tables](#) [Figures](#)
- [◀](#) [▶](#)
- [◀](#) [▶](#)
- [Back](#) [Close](#)
- [Full Screen / Esc](#)
- [Printer-friendly Version](#)
- [Interactive Discussion](#)

Aerosol mass spectrometer constraint on the global SOA budget

D. V. Spracklen et al.

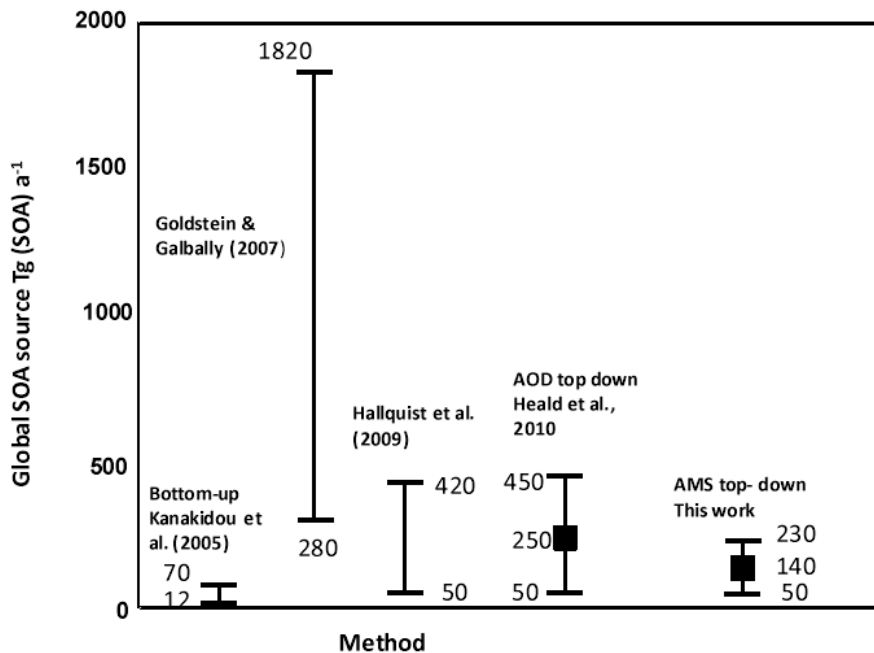


Fig. 13. Comparison of the global budget of SOA calculated here with previous work (we convert the OA source from Heald et al. (2010) into an SOA source assuming a 2:1 OA:OC conversion and the POA emissions used in this study).

[Title Page](#) | [Abstract](#) | [Introduction](#)
[Conclusions](#) | [References](#)
[Tables](#) | [Figures](#)
[◀](#) | [▶](#)
[◀](#) | [▶](#)
[Back](#) | [Close](#)
[Full Screen / Esc](#)

[Printer-friendly Version](#)

[Interactive Discussion](#)